



This is a repository copy of *Measurements of the suppression and correlations of dijets in Xe+Xe collisions at $\sqrt{s_{NN}}=5.44$ TeV.*

White Rose Research Online URL for this paper:

<https://eprints.whiterose.ac.uk/205917/>

Version: Published Version

Article:

Aad, G. orcid.org/0000-0002-6665-4934, Abbott, B. orcid.org/0000-0002-5888-2734, Abeling, K. orcid.org/0000-0002-1002-1652 et al. (2898 more authors) (2023) Measurements of the suppression and correlations of dijets in Xe+Xe collisions at $\sqrt{s_{NN}}=5.44$ TeV. *Physical Review C*, 108 (2). 024906. ISSN 2469-9985

<https://doi.org/10.1103/physrevc.108.024906>

Reuse

This article is distributed under the terms of the Creative Commons Attribution (CC BY) licence. This licence allows you to distribute, remix, tweak, and build upon the work, even commercially, as long as you credit the authors for the original work. More information and the full terms of the licence here:


<https://creativecommons.org/licenses/>

Takedown

If you consider content in White Rose Research Online to be in breach of UK law, please notify us by emailing eprints@whiterose.ac.uk including the URL of the record and the reason for the withdrawal request.



eprints@whiterose.ac.uk
<https://eprints.whiterose.ac.uk/>

Measurements of the suppression and correlations of dijets in Xe+Xe collisions at $\sqrt{s_{NN}} = 5.44$ TeVG. Aad *et al.**
(ATLAS Collaboration) (Received 9 February 2023; accepted 14 July 2023; published 9 August 2023)

Measurements of the suppression and correlations of dijets is performed using $3 \mu\text{b}^{-1}$ of Xe+Xe data at $\sqrt{s_{NN}} = 5.44$ TeV collected with the ATLAS detector at the CERN Large Hadron Collider. Dijets with jets reconstructed using the $R = 0.4$ anti- k_r algorithm are measured differentially in jet p_T over the range of 32 to 398 GeV and the centrality of the collisions. Significant dijet momentum imbalance is found in the most central Xe+Xe collisions, which decreases in more peripheral collisions. Results from the measurement of per-pair normalized and absolutely normalized dijet p_T balance are compared with previous Pb+Pb measurements at $\sqrt{s_{NN}} = 5.02$ TeV. The differences between the dijet suppression in Xe+Xe and Pb+Pb are further quantified by the ratio of pair nuclear-modification factors. The results are found to be consistent with those measured in Pb+Pb data when compared in classes of the same event activity and when taking into account the difference between the center-of-mass energies of the initial parton scattering process in Xe+Xe and Pb+Pb collisions. These results should provide input for a better understanding of the role of energy density, system size, path length, and fluctuations in the parton energy loss.

DOI: [10.1103/PhysRevC.108.024906](https://doi.org/10.1103/PhysRevC.108.024906)**I. INTRODUCTION**

A major focus of relativistic heavy-ion physics is to study the quark-gluon plasma (QGP), a hot and dense medium composed of deconfined quarks and gluons. During the initial stages of heavy-ion collisions, hard-scattering interactions between constituents of incoming nuclei may occur. In leading-order calculations in perturbative quantum chromodynamics, two high transverse momenta (p_T) partons (quarks and/or gluons) are produced in these interactions. These partons then fragment and hadronize to form two jets that are oriented back to back in azimuth. When traversing the QGP, these jets suffer radiative and collisional energy loss leading to a phenomenon known as jet quenching [1,2]. Jet quenching has been observed and quantified in many measurements at the BNL Relativistic Heavy Ion Collider (RHIC) and the CERN Large Hadron Collider (LHC) (for a recent review see Ref. [3]), but the theoretical understanding of partonic interactions and properties of the QGP is still incomplete.

A basic observable quantifying the impact of jet quenching on inclusive jets is the jet nuclear-modification factor, R_{AA} [4–6]. A factor-of-2 suppression of inclusive jet production in central Pb + Pb collisions compared to the production in pp collisions is seen in measurements of R_{AA} . While measurements of inclusive jet suppression contain contributions from jets traversing different path lengths in the QGP and suffering differently from jet quenching fluctuations, the measurements

of dijets provide additional new information. The increase in the number of strongly asymmetric dijets may be directly connected with the different path lengths of the two jets in the medium [7]. The compound effect of fluctuations in the vacuumlike fragmentation pattern and medium related fluctuations in the energy loss may also significantly contribute to the measured asymmetry [8].

Dijet suppression in Pb + Pb collisions was measured in terms of the momentum balance [9–13] and the pair nuclear-modification factor [13], which quantified the differences between the suppression of the leading (in transverse momentum) jet and the subleading jet (opposite in azimuth).

So far, only inclusive charged-hadron suppression was measured in Xe+Xe collisions [14–16], while the parton energy-loss measurements involving jets and dijets at the LHC have only been performed in Pb + Pb collisions. The 2017 LHC Xe+Xe run provides a possibility to study jet quenching in collisions of nuclei lighter than Pb, which is attractive for several reasons. First, the underlying event (UE) in the most central collisions, where the collision geometry is the most symmetric, is smaller in Xe+Xe collisions than in Pb + Pb collisions. Secondly, the decrease in the number of nucleons or the nuclear radius between Pb and Xe nuclei may affect the amount of jet quenching through a reduction in both the overall energy density and the path lengths traversed by the hard-scattered partons in the medium. Consequently, measurements of dijets in different collision systems should further constrain the impact of the path length, energy density, and fluctuations on the jet quenching. Studying the parton energy loss in a collision system that is smaller than the Pb + Pb system may also help to predict the energy loss for oxygen-oxygen collisions, which are intended to be performed during LHC Run 3 [17]. This paper reports the first measurement of jet suppression for Xe+Xe collisions.

*Full author list given at the end of the article.

Published by the American Physical Society under the terms of the [Creative Commons Attribution 4.0 International](https://creativecommons.org/licenses/by/4.0/) license. Further distribution of this work must maintain attribution to the author(s) and the published article's title, journal citation, and DOI.

The analysis presented here follows closely the techniques that were used to measure dijets in Pb+Pb collisions [13]. The highest p_T jet in the event, the leading jet, and the second highest p_T jet, the subleading jet, are studied. The leading jet transverse momentum, $p_{T,1}$ is required to be greater than 100 GeV and the subleading jet transverse momentum, $p_{T,2}$, greater than 32 GeV. Both the jets are required to be in the rapidity¹ region $|y| < 2.1$. The subleading jet is required to be on the opposite side in azimuth from the leading jet, which is defined by the condition $\Delta\phi = |\phi_1 - \phi_2| > 7\pi/8$. The momentum balance between the leading and subleading jet is quantified by the ratio

$$x_J = \frac{p_{T,2}}{p_{T,1}}.$$

The distribution of x_J can be normalized by the number of dijets (N_{pair}),

$$\frac{1}{N_{\text{pair}}} \frac{dN_{\text{pair}}}{dx_J}, \quad (1)$$

which is called *per-pair normalized* momentum-imbalance distribution. Alternatively, the distribution can be normalized by the effective heavy-ion luminosity,

$$\frac{1}{N_{\text{evt}}} \frac{1}{\langle T_{AA} \rangle} \frac{dN_{\text{pair}}}{dx_J}, \quad (2)$$

which is called the *absolutely normalized* momentum-imbalance distribution, where $\langle T_{AA} \rangle$ is the average nuclear-thickness function and N_{evt} is the number of minimum bias events in a given centrality interval. The absolutely normalized momentum-imbalance distribution allows the differences between the yields of dijets with a given dijet momentum-imbalance in different collision centrality intervals to be directly quantified. Both the per-pair normalized and absolutely normalized dijet momentum-imbalance distributions were previously measured in Pb + Pb collisions [13]. The dijet yields in Xe+Xe collisions are also extracted to calculate the pair nuclear-modification factors for leading and subleading jets. Measurements made in Xe+Xe collisions are compared with those obtained for Pb + Pb collisions.

II. ATLAS DETECTOR AND TRIGGER

The ATLAS detector [18] at the LHC covers nearly the full solid angle around the nominal interaction point. It contains

¹ATLAS uses a right-handed coordinate system with its origin at the nominal interaction point (IP) in the center of the detector and the z axis along the beam pipe. The x axis points from the IP to the center of the LHC ring, and the y axis points upward. Cylindrical coordinates (r, ϕ) are used in the transverse plane, ϕ being the azimuthal angle around the z axis. The pseudorapidity is defined in terms of the polar angle θ as $\eta = -\ln \tan(\theta/2)$ and the rapidity is defined in terms of the energy E and z component of the momentum, p_z , as $y = 1/2 \ln[(E + p_z)/(E - p_z)]$. Transverse momentum and transverse energy are defined as $p_T = p \sin(\theta)$ and $E_T = E \sin(\theta)$, respectively. The angular distance between two objects with relative differences $\Delta\eta$ in pseudorapidity and $\Delta\phi$ in azimuth is given by $\Delta R = \sqrt{(\Delta\eta)^2 + (\Delta\phi)^2}$.

an inner tracking detector (ID) surrounded by a thin superconducting solenoid, electromagnetic and hadronic calorimeters, a zero-degree calorimeter, and a muon spectrometer that incorporates three large superconducting toroidal magnets. The inner-detector system is immersed in a 2 T axial magnetic field and provides charged-particle tracking in the range of $|\eta| < 2.5$ with 2π coverage in azimuth. The ATLAS calorimeter system covers the pseudorapidity range of $|\eta| < 4.9$. In the region of $|\eta| < 3.2$, the electromagnetic calorimetry is provided by both barrel and endcap high-granularity lead-liquid-argon (LAr) calorimeters, with an additional thin LAr presampler covering $|\eta| < 1.8$, to enable corrections for energy lost in material upstream of the calorimeters. Hadronic calorimetry is provided by a steel scintillating-tile calorimeter that is segmented into three barrel structures with $|\eta| < 1.7$, and two copper-LAr hadronic endcap calorimeters. To complete the solid angle coverage, forward ($3.2 < |\eta| < 4.9$) copper-LAr and tungsten-LAr calorimeter modules (FCal) are used, optimized for electromagnetic and hadronic measurements, respectively.

Data are recorded with a multistage trigger system [19]. Events are selected using hardware-based first-level triggers (L1) implemented in custom electronics, and then processed by a high-level trigger (HLT) to further reduce the accepted event rate and provide additional purity.

An extensive software suite [20] is used in data simulation, in the reconstruction and analysis of real and simulated data, in detector operations, and in the trigger and data acquisition systems of the experiment.

III. DATA SELECTION AND MONTE CARLO SIMULATION SAMPLES

The analysis uses data from $^{129}\text{Xe} + ^{129}\text{Xe}$ collisions at $\sqrt{s_{NN}} = 5.44$ TeV collected in 2017 at the LHC with a total integrated luminosity of $3 \mu\text{b}^{-1}$. Events were recorded using a combination of two triggers designed to select minimum-bias (MB) collisions, which allows measured jets to be reconstructed with full efficiency. These triggers require the total transverse energy deposited in the calorimeters at L1 to be more than 4 GeV or, if the total transverse energy at L1 is less than 4 GeV, then the presence of at least one track reconstructed in the ID is required.

In addition to the trigger selections, events are required to have a reconstructed primary vertex and satisfy criteria that ensure stable detector conditions. A few recorded events ($\approx 0.1\%$) consistent with two Xe+Xe interactions in the same bunch crossing (pileup) are removed based on the tight correlation between the sum of the total transverse energy in the forward calorimeter (ΣE_T^{FCal}) and the number of reconstructed tracks matched to the primary vertex.

The level of overall event activity or ‘‘centrality,’’ which is indicative of the degree of overlap between the two colliding nuclei, is characterized using ΣE_T^{FCal} measured at the electromagnetic scale [21]. The Glauber model [22] is used to obtain a correspondence between the ΣE_T^{FCal} distribution and the fraction of the total inelastic Xe+Xe cross section, allowing the setting of the centrality percentiles [23,24]. A Glauber model analysis was also applied to relate quantiles of

TABLE I. The centrality intervals in Xe+Xe collisions and their corresponding $\langle T_{AA} \rangle$ values with their respective absolute uncertainties.

Centrality	$\langle T_{AA}^{\text{Xe+Xe}} \rangle$ (mb ⁻¹)
0–10%	12.38 ± 0.08
10–20%	7.53 ± 0.09
20–40%	3.52 ± 0.09
40–80%	0.630 ± 0.036

the ΣE_T^{FCal} distribution to geometric properties of the collision such as $\langle T_{AA} \rangle$. Centrality intervals in Xe+Xe collisions used in the analysis along with $\langle T_{AA} \rangle$ are summarized in Table I. The comparison of Xe+Xe and Pb+Pb results is performed in the same centrality intervals, covering the centrality range 0–80% as listed in Table I. In addition, the results for both systems are also compared by selecting events with similar activity, quantified by ΣE_T^{FCal} . For this comparison, events in Xe+Xe collisions are selected in intervals of ΣE_T^{FCal} matching the ΣE_T^{FCal} intervals in Pb+Pb collisions that correspond to the Pb+Pb centrality intervals of 10–20%, 20–40% and 40–60% used in Ref. [13]. The corresponding Xe+Xe centrality intervals are summarized in Table II.

Monte Carlo (MC) simulations are used to understand the performance of the ATLAS detector in high occupancy Xe+Xe data samples and to correct the data for detector effects. A sample of 9×10^6 pp jet events was generated using PYTHIA8 [25] at $\sqrt{s} = 5.44$ TeV with the A14 set of tuned parameters [26] and the NNPDF23LO parton distribution functions [27]. To correctly describe the UE of Xe+Xe collisions, these generated MC events were overlaid onto events from a dedicated sample of minimum-bias Xe+Xe data. The detector response was simulated [20] using GEANT4 [28,29]. A pp MC sample of 2.4×10^6 jet events with the same settings but at $\sqrt{s} = 5.02$ TeV was also generated to determine the correction for the difference between the center-of-mass energies in Xe+Xe and Pb+Pb collisions. In addition, samples of jet events using HERWIG++ [30] with the UEEE5 tune [31] and the CTEQ6L1 parton distribution functions [32] were generated to assess systematic uncertainties.

IV. JET RECONSTRUCTION

The jet reconstruction procedure follows that used by ATLAS for previous jet measurements in Pb+Pb collisions described in Ref. [33], including the UE subtraction procedure. Jets are reconstructed using the anti- k_r algorithm [34] with radius parameter $R = 0.4$ implemented in the FASTJET

software package [35]. Jets are formed by clustering calorimetric towers of angular size $\Delta\eta \times \Delta\phi = 0.1 \times \pi/32$. The energy in the tower is obtained by summing the energies deposited in calorimeter cells at the electromagnetic energy scale within the tower boundaries. An η - and ϕ -dependent UE subtraction is performed for each calorimeter tower within the jet using an iterative procedure, where the background due to the UE is modulated to account for the effects of hydrodynamic flow [36]. Then, jet η and p_T -dependent correction factors derived from simulations are applied to the measured jet energy to correct for the calorimeter energy response [37]. This calibration is followed by a cross-calibration that relates the jet energy scale of jets reconstructed by the procedure outlined above to the jet energy scale in 13 TeV pp collisions [38]. An additional correction based on *in situ* studies of jets recoiling against photons, Z bosons, and jets in other regions of the calorimeters is applied [39].

Jets are defined at the generator level in the MC sample before detector simulation by applying the anti- k_r algorithm with $R = 0.4$ to stable particles with a proper lifetime greater than 30 ps, but excluding muons and neutrinos, which do not leave significant energy deposits in the calorimeter. After the detector simulation, the generator-level jets are matched to the nearest reconstructed jet within $\Delta R = 0.4$.

The performance of the jet reconstruction is shown in Fig. 1 in terms of the jet energy scale (JES) and jet energy resolution (JER), which correspond to the mean and width of the jet response ($p_T^{\text{reco}}/p_T^{\text{truth}}$), where p_T^{reco} and p_T^{truth} are the reconstructed and generator level jet transverse momenta, respectively. The maximum departure of the JES from unity in the inclusive jet sample is 8% in peripheral collisions (40–80% centrality) for $p_T^{\text{truth}} < 50$ GeV. For $p_T^{\text{truth}} > 50$ GeV the JES is consistent with unity within 1%. A similar performance of the JES is seen in Pb+Pb collisions [13]. Contributions to the JER can be factorized into three terms, $\frac{a}{\sqrt{p_T}} \oplus \frac{b}{p_T} \oplus c$, where the constants a , b , and c quantify the magnitude of stochastic term, noise term, and constant term, respectively. The stochastic and constant terms are related to the calorimeter response to the showering process while the noise term constitutes the centrality-dependent part of JER that is driven by the p_T -independent UE fluctuations [40]. The JER is largest in 0–10% central collisions where $b = 11.3 \pm 0.1$ GeV, which is about 3 GeV smaller than the value of b in 0–10% central Pb+Pb collisions but similar to the value of b in 10–20% central Pb+Pb collisions [4]. Constants a and c are found to be consistent between Xe+Xe and Pb+Pb collisions. The impact of the small departure of the JES from unity on measured quantities and the impact of the JER is corrected for by the unfolding procedure.

TABLE II. The centrality intervals in Xe+Xe and Pb+Pb collisions for matching ΣE_T^{FCal} intervals and respective $\langle T_{AA} \rangle$ values for Xe+Xe collisions.

Xe+Xe cent.	Pb+Pb cent.	$\langle T_{AA}^{\text{Xe+Xe}} \rangle$ (mb ⁻¹)	ΣE_T^{FCal} (TeV)
0–7.7%	10–20%	13.05 ± 0.08	2.06–3.00
7.7–29.9%	20–40%	6.45 ± 0.09	0.89–2.06
29.9–53.2%	40–60%	1.81 ± 0.07	0.30–0.89

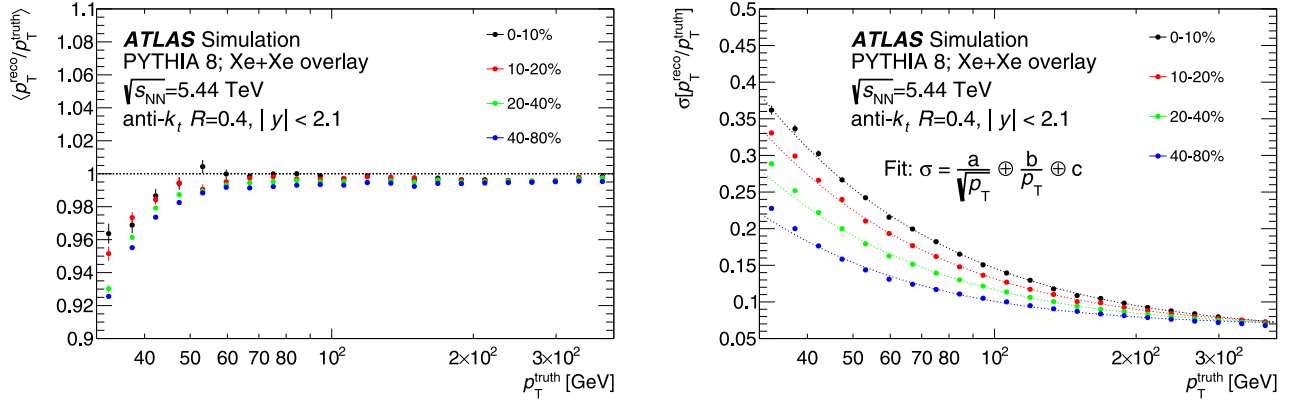


FIG. 1. The performance of (left) the JES and (right) the JER for jets with $|y| < 2.1$ evaluated as a function of p_T^{truth} in different centrality bins. The right plot includes JER fits shown with dashed curves (for details, see the text). Simulated hard scatter events were overlaid onto events from a dedicated sample of minimum-bias Xe+Xe data.

V. DATA ANALYSIS

The analysis is performed using the same methods as described in Ref. [13]. Jet pairs are formed from the two highest- p_T jets in the event. Jet pairs not fulfilling the selection criteria for leading and subleading jet defined in Sec. I are not used.

The distributions of dijet momentum-imbalance and the pair nuclear-modification factor are not calculated directly. They are obtained in the final step of the analysis from two-dimensional $(p_{T,1}, p_{T,2})$ distributions. The binning of $(p_{T,1}, p_{T,2})$ distributions follows a logarithmic distribution with 32 intervals between $p_T = 10$ GeV and $p_T = 398$ GeV. This binning allows the same intervals to be selected as those used in the previous dijet and inclusive jet measurements in Pb+Pb collisions [4,13]. Distributions are measured in the p_T range of 32–398 GeV. Bins with $p_T < 32$ GeV are only used in MC simulation as underflow bins in the unfolding procedure. The maximum value of 398 GeV is determined by the absence of jets with $p_T > 398$ GeV in the data. In total, 14 325 dijets were analyzed in the full centrality range 0–80%.

The $(p_{T,1}, p_{T,2})$ distributions are corrected for the background from jet pairs not originating in the same hard process and from spurious jets from fluctuations of the UE. This combinatoric background is estimated from the data using the yield of dijets with angular separation $1.0 < \Delta\phi < 1.4$ from the leading jet. This angular requirement minimizes the contribution from real dijets, which have a maximum at $\Delta\phi = \pi$, and contributions from split jets in the vicinity of $\Delta\phi \approx 0.4$. The background jet yield is then subtracted from the yield of dijets with $\Delta\phi > 7\pi/8$. This correction is largest in the most central collisions and at low p_T . In the 0–10% centrality region, for $p_{T,1} > 100$ GeV and $32 < p_{T,2} < 50$ GeV, it subtracts up to 15% of the dijets while for all other p_T and centrality bins the correction subtracts less than 4% of the dijets. The presence of background jets may create a situation where such a jet has higher p_T than the real subleading jet. This background jet would then be falsely identified as the subleading jet and this would cause oversubtraction leading to inefficiency. The background-subtracted $(p_{T,1}, p_{T,2})$ distri-

butions are corrected for this effect. The efficiency correction is estimated from the per-event rate of inclusive jets in data using the same procedure as described in Ref. [12]. After the background of size B is subtracted from the raw yields N^{raw} , the efficiency ϵ is applied using the formula $N^{\text{corr}} = (N^{\text{raw}} - B)/\epsilon$, where N^{corr} is the final yield that goes into the unfolding. The efficiency correction is largest in the most central collisions at the lowest $p_{T,2}$ values, where it reaches 3%. For subleading jets with $p_{T,2} > 50$ GeV the efficiency correction is smaller than 1%.

After the combinatoric background-subtraction and efficiency correction, the $(p_{T,1}, p_{T,2})$ distributions are unfolded for the detector response using the Bayesian unfolding implemented in the ROOUNFOLD package [41,42]. The four-dimensional response matrices are filled symmetrically in reconstruction- and generator-level $(p_{T,1}, p_{T,2})$ to include the possibility that the leading and subleading jets are swapped due to resolution effects. Generator-level jets entering the response matrix satisfy the same y and $\Delta\phi$ conditions, but extend the minimum p_T to lower values ($p_{T,1} > 20$ GeV and $p_{T,2} > 10$ GeV) to account for the migration of jets in and out of the kinematic fiducial region. The unfolding procedure also corrects the jet reconstruction inefficiency when the reconstructed jet pair is lost due to resolution effects but the corresponding generator-level jet pair exists. The response matrices are reweighted in generator-level, $(p_{T,1}, p_{T,2})$ by smooth ratios of the $(p_{T,1}, p_{T,2})$ distributions in data to those in the reconstructed MC sample such that the $(p_{T,1}, p_{T,2})$ distributions in the response matrices better represent those in the data.

The number of iterations in the unfolding is chosen to be three for all the centrality intervals, which optimizes the balance between the statistical uncertainty and systematic bias introduced by the shapes of the distributions used to construct the response matrix. The statistical uncertainty is estimated by performing 100 unfoldings where each bin in input data and each bin in the response matrix are varied separately according to their corresponding statistical uncertainties. The standard deviation of these is evaluated in each bin and used as the estimate of the statistical uncertainty. The two values,

one from the statistical uncertainty in the data and one from the statistical uncertainty in the response matrix, are summed in quadrature to obtain the total statistical uncertainty in the unfolded distributions.

The unfolded $(p_{T,1}, p_{T,2})$ distributions are used to calculate the resulting one-dimensional dijet momentum-imbalance distributions defined in Eqs. (1) and (2). The unfolded $(p_{T,1}, p_{T,2})$ is mapped to the region $p_{T,2} \leq p_{T,1}$ and diagonally sliced to project the x_j distribution as described in Ref. [13]. The x_j bin boundaries are defined by the previously discussed logarithmic binning in transverse momentum. The x_j distributions measured in Xe+Xe collisions can be directly compared with distributions measured in Pb+Pb collisions. This comparison may be affected by the difference between the cross sections, due to the different center-of-mass energies of the initial hard process scattering, in Xe+Xe and Pb+Pb collisions. To quantify this difference, the factor $\mathcal{C}(x_j)$ is calculated as a ratio of PYTHIA8 x_j distributions in 5.44 TeV pp collisions to the same quantity in simulated 5.02 TeV pp collisions,

$$\mathcal{C}(x_j) = \frac{1/N dN_{\text{PYTHIA8}}^{\text{pair}}(pp, 5.44 \text{ TeV})/dx_j}{1/N dN_{\text{PYTHIA8}}^{\text{pair}}(pp, 5.02 \text{ TeV})/dx_j}. \quad (3)$$

The normalization N is N_{pair} and $N_{\text{evt}}\langle T_{AA} \rangle$ for per-pair normalized and absolutely normalized distributions, respectively.

The $\mathcal{C}(x_j)$ factor can be used to scale the x_j distributions measured in Pb+Pb data. For the absolutely normalized x_j distributions, the magnitude of $\mathcal{C}(x_j)$ ranges from 1.25 at low x_j values to 1.15 at x_j values approaching unity. For per-pair normalized x_j distributions, the magnitude of $\mathcal{C}(x_j)$ is consistent with unity and it is not applied on per-pair normalized x_j distributions. Similar scaling was also applied in other analyses using 5.44 TeV Xe+Xe data [14,15].

The unfolded $(p_{T,1}, p_{T,2})$ distributions are also projected onto the $p_{T,1}$ and $p_{T,2}$ axes to construct the pair nuclear-modification factors for dijets as a function of the leading jet p_T ,

$$R_{AA}^{\text{pair}}(p_{T,1}) = \frac{\frac{1}{\langle T_{AA} \rangle N_{\text{evt}}^{AA}} \int_{0.32 \times p_{T,1}}^{p_{T,1}} \frac{d^2 N^{\text{pair}}(AA)}{dp_{T,1} dp_{T,2}} dp_{T,2}}{\frac{1}{\mathcal{L}_{pp}} \int_{0.32 \times p_{T,1}}^{p_{T,1}} \frac{d^2 N^{\text{pair}}(pp)}{dp_{T,1} dp_{T,2}} dp_{T,2}},$$

and as a function of subleading jet p_T ,

$$R_{AA}^{\text{pair}}(p_{T,2}) = \frac{\frac{1}{\langle T_{AA} \rangle N_{\text{evt}}^{AA}} \int_{p_{T,2}}^{p_{T,2}/0.32} \frac{d^2 N^{\text{pair}}(AA)}{dp_{T,1} dp_{T,2}} dp_{T,1}}{\frac{1}{\mathcal{L}_{pp}} \int_{p_{T,2}}^{p_{T,2}/0.32} \frac{d^2 N^{\text{pair}}(pp)}{dp_{T,1} dp_{T,2}} dp_{T,1}}. \quad (4)$$

Here \mathcal{L}_{pp} is the integrated luminosity of pp collisions and the boundaries in the integrals are given by the measured minimum value of x_j .

To evaluate the differences between the dijet quenching in Xe+Xe and Pb+Pb collisions the ratio of pair nuclear-modification factors for the leading jet is defined as

$$\rho_{\text{Xe,Pb}}(p_{T,1}) = \frac{R_{AA}^{\text{pair}}(p_{T,1})|_{\text{Xe+Xe}}}{R_{AA}^{\text{pair}}(p_{T,1})|_{\text{Pb+Pb}}} = \frac{\frac{1}{\langle T_{AA}^{\text{Xe+Xe}} \rangle N_{\text{evt}}^{\text{Xe+Xe}}} \int_{0.32 \times p_{T,1}}^{p_{T,1}} \frac{d^2 N^{\text{pair}}(\text{Xe+Xe}, 5.44 \text{ TeV})}{dp_{T,1} dp_{T,2}} dp_{T,2}}{\mathcal{C}(p_{T,1}) \times \frac{1}{\langle T_{AA}^{\text{Pb+Pb}} \rangle N_{\text{evt}}^{\text{Pb+Pb}}} \int_{0.32 \times p_{T,1}}^{p_{T,1}} \frac{d^2 N^{\text{pair}}(\text{Pb+Pb}, 5.02 \text{ TeV})}{dp_{T,1} dp_{T,2}} dp_{T,2}}. \quad (5)$$

As there is no reference pp data at 5.44 TeV, the factor $\mathcal{C}(p_{T,1})$ is introduced to account for the difference between the center-of-mass energies of 5.44 and 5.02 TeV collision data. It is evaluated using PYTHIA8 Monte Carlo simulations as

$$\mathcal{C}(p_{T,1}) = \frac{\int_{0.32 \times p_{T,1}}^{p_{T,1}} \frac{d^2 N_{\text{PYTHIA8}}^{\text{pair}}(pp, 5.44 \text{ TeV})}{dp_{T,1} dp_{T,2}} dp_{T,2}}{\int_{0.32 \times p_{T,1}}^{p_{T,1}} \frac{d^2 N_{\text{PYTHIA8}}^{\text{pair}}(pp, 5.02 \text{ TeV})}{dp_{T,1} dp_{T,2}} dp_{T,2}}. \quad (6)$$

Analogously, the ratio of pair nuclear-modification factors for subleading jets, $\rho_{\text{Xe,Pb}}(p_{T,2})$, and the factor $\mathcal{C}(p_{T,2})$ can be defined using Eq. (4). The magnitude of the \mathcal{C} factor ranges from 1.12 at 32 GeV to 1.31 at 398 GeV for both leading and subleading jets. The ratios $\rho_{\text{Xe,Pb}}(p_{T,1})$ and $\rho_{\text{Xe,Pb}}(p_{T,2})$ allow the differences between the jet quenching in Xe+Xe and Pb+Pb collisions to be directly quantified.

VI. SYSTEMATIC UNCERTAINTIES

Systematic uncertainties arise from uncertainties in the JES, JER, background subtraction procedures, $\langle T_{AA} \rangle$ values, the unfolding weight selection, minimum $p_{T,2}$ lower boundary, and from the unfolding procedure performance observed in the MC sample. For each source of systematic uncertainty, except for the uncertainty in $\langle T_{AA} \rangle$ and unfolding nonclosure, the entire analysis is repeated by varying the response matrix according to the systematic uncertainties.

The difference between the final distributions of the baseline measurement and the measurement with varied values is used as the estimate of the systematic uncertainty. For the $\rho_{\text{Xe,Pb}}$, the JES and JER systematic uncertainties are correlated between Xe+Xe and Pb+Pb, while all the other uncertainties are taken as uncorrelated.

The systematic uncertainty in the JES has four components. The first, centrality-independent component is determined from *in situ* studies of the calorimeter response to jets reconstructed with the procedure used in 13 TeV pp collisions [21,43]. The second component accounts for the relative energy-scale difference between the jet reconstruction procedures used in this analysis and those used for 13 TeV pp collisions [38]. The third component accounts for possible mismodeling of the relative abundances of quark and gluon jets and the calorimeter response to them in the MC simulation. This is assessed by comparing quark and gluon jets generated with PYTHIA and with HERWIG++. The fourth

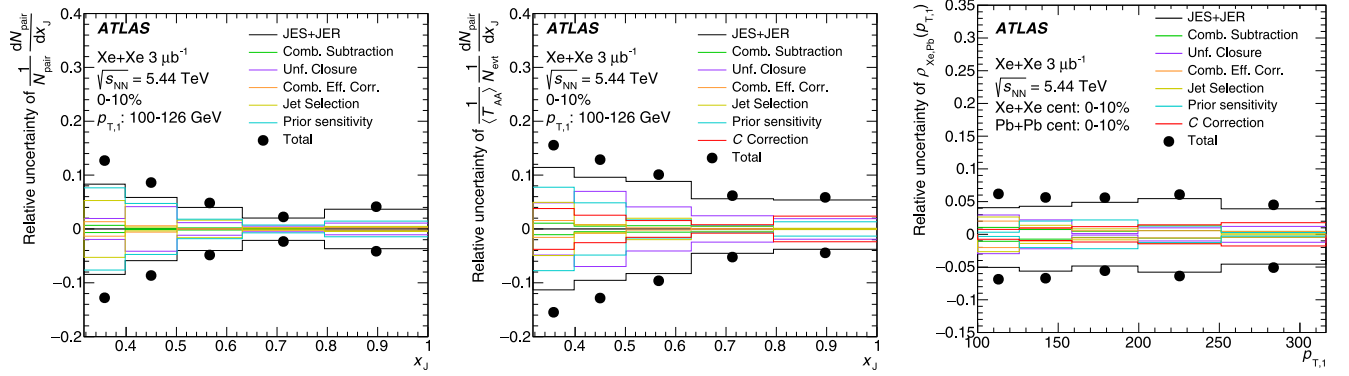


FIG. 2. The relative magnitude of systematic uncertainties for (left) the per-pair normalized x_j distribution, (middle) the absolutely normalized x_j distribution, and (right) the $\rho_{Xe,Pb}(p_{T,1})$, all in the 0–10% centrality interval.

component is centrality dependent and accounts for any incomplete knowledge of the calorimetric response to quenched jets through modifications of parton showering [38,44]. The total size of systematic uncertainty from the JES is approximately 1–8% with the maximum around $x_j \approx 0.32$ in 0–10% central collisions. It decreases with x_j except for the last centrality interval where it increases, reaching a value of about 2%. For the $\rho_{Xe,Pb}$, the largest systematic uncertainty from the JES is 5% and it exhibits only a weak p_T dependence.

The systematic uncertainty in the JER has two components. The first component is evaluated using an *in situ* technique for 13 TeV pp data that involves studies of dijet energy balance [45,46]. The second component accounts for differences between the tower-based jet reconstruction and the jet reconstruction used in the analyses of 13 TeV pp data and the differences between the calibration procedures. Both of these uncertainties are applied via the smearing factor that is used to include an additional contribution to the resolution of the reconstructed p_T in the MC sample by the Gaussian smearing procedure. This modified reconstructed p_T enters the response matrices that are used to derive the alternative result. The uncertainty from the JER is approximately 10% for $x_j \approx 0.32$ in 0–10% central collisions and decreases with x_j except for the last two intervals in x_j where it increases to about 5%. For $\rho_{Xe,Pb}$, the largest systematic uncertainty from the JER is 2% and exhibits only a weak p_T dependence. The smaller JER uncertainty in $\rho_{Xe,Pb}$ compared with the JES is due to a correlation with the Pb+Pb uncertainties.

The systematic uncertainty arising from the removal of the combinatoric jet background procedure has two components. The first component is connected with the determination of the yield of combinatoric background jets and is determined using an alternative sideband of $1.1 < \Delta\phi < 1.5$ following the procedure described in Ref. [12]. The second contribution is associated with the determination of the efficiency correction and is determined from the difference between the analysis performed with and without the efficiency correction. These uncertainties do not dominate the overall systematic uncertainty. The largest values of the uncertainty due to the determination of combinatoric jet background and the uncertainty due to the efficiency correction are about 1% and 2%, respectively, for both the x_j and $\rho_{Xe,Pb}$ distributions.

The uncertainty in $\langle T_{AA} \rangle$ arises from geometric modeling uncertainties (e.g., nucleon-nucleon inelastic cross section, Woods-Saxon parametrization of the nucleon distribution [47,48]) and the uncertainty of the fraction of selected inelastic Xe+Xe collisions. This uncertainty only affects the overall normalization and is independent of the dijet kinematics. The values of the uncertainties in $\langle T_{AA} \rangle$ for Xe+Xe are shown in Tables I and II. This uncertainty is uncorrelated between Xe+Xe and Pb+Pb [13].

There are two sources of systematic uncertainty connected with the unfolding procedure. The first one arises from the imprecision in the determination of the initial distributions used in the iterative procedure for the underlying generator-level distribution in the unfolding procedure. This uncertainty is calculated from the difference between the unfolded distributions constructed using the nominal reweighted prior and the prior without applying the reweighting. The second source derives from the sensitivity of the unfolding procedure to the jet selection choice of the minimum jet p_T . This is estimated by changing the minimum jet p_T from 32 to 25 GeV. To perform a check on the performance of the full analysis procedure a closure test is performed with the MC sample by evaluating the differences between the final unfolded distributions and the generator-level distributions of the MC sample. The difference from unity in the closure test is included as the additional source of systematic uncertainty. These uncertainties are the largest at low x_j , where the uncertainty due to the prior sensitivity reaches 10% for $100 < p_{T,1} < 126$ GeV in 0–10% central collisions. For larger x_j and p_T they decrease to 1–3%.

The uncertainty in the $\mathcal{C}(p_T)$ factors defined in Sec. V is estimated as the difference between the $\mathcal{C}(p_T)$ factors evaluated using PYTHIA8 and HERWIG++ MC samples. The magnitude of the uncertainty in the \mathcal{C} factor stays below 2% over the full p_T range of the $\rho_{Xe,Pb}$ distribution. The uncertainty in the $\mathcal{C}(x_j)$ factor is evaluated in the same way as the uncertainty in the $\mathcal{C}(p_T)$ factors. Its magnitude stays below 2%, and it is applied as the additional uncertainty in the Pb+Pb x_j distributions.

The magnitude of systematic uncertainties for per-pair normalized dijet momentum-imbalance, absolutely normalized dijet momentum-imbalance, and for the $\rho_{Xe,Pb}(p_{T,1})$

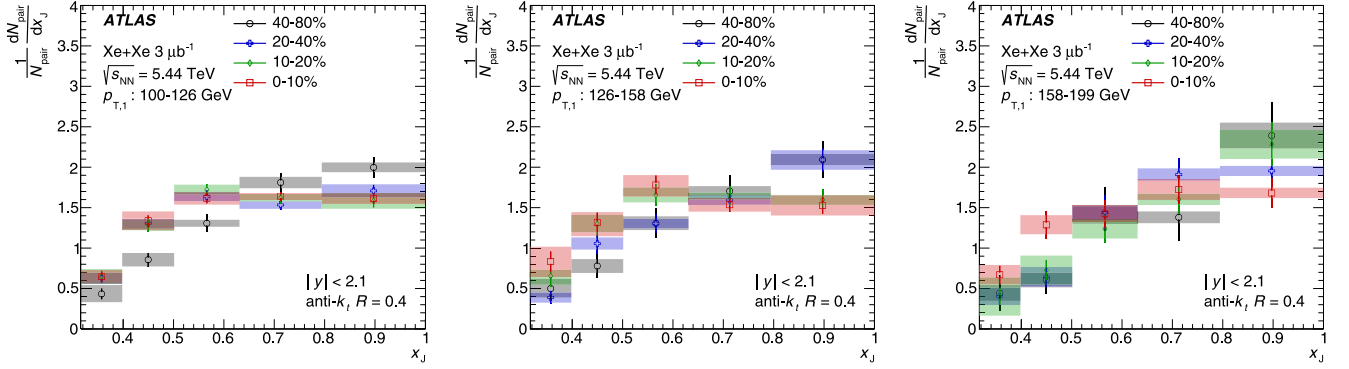


FIG. 3. Per-pair normalized x_j distribution evaluated in four centrality intervals and three $p_{T,1}$ intervals of leading jet p_T : (left) $100 < p_{T,1} < 126$ GeV, (middle) $126 < p_{T,1} < 158$ GeV, and (right) $158 < p_{T,1} < 199$ GeV. Statistical and systematic uncertainties are represented by error bars and boxes, respectively.

distributions, in the most central collisions, is shown in Fig. 2.

VII. RESULTS

Figure 3 shows the per-pair normalized distribution of x_j evaluated in four centrality intervals (0–10%, 10–20%, 20–40%, and 40–80%) and three p_T intervals of the leading jet p_T ($100 < p_{T,1} < 126$ GeV, $126 < p_{T,1} < 158$ GeV, and $158 < p_{T,1} < 199$ GeV). A substantial difference between the shape of x_j distribution in the most central collisions (0–10%) and the most peripheral collisions (40–80%) is seen. In peripheral collisions, the most frequent configurations are balanced dijets, while in central collisions the rate of imbalanced dijets is the same or higher than the rate of balanced dijets. These features are also observed in Pb+Pb collisions [13]. Narrowing of the x_j distribution with increasing $p_{T,1}$, previously measured in Pb+Pb collisions, is not that pronounced in the measured p_T interval in Xe+Xe collisions. The peak structure at $x_j = 0.6$, previously measured in 0–10% Pb+Pb collisions, is not present in 0–10% Xe+Xe collisions. This may be connected with a smaller overlapping region of colliding nuclei in Xe+Xe compared with Pb+Pb collisions. The evo-

lution between the central and peripheral Xe+Xe collisions is not as pronounced as in Pb+Pb collisions. The absence of a clearly visible evolution is connected with a worse statistical precision of the Xe+Xe measurement compared with the Pb+Pb measurement.

Figure 4 shows the absolutely normalized distribution of x_j evaluated for the same centrality and $p_{T,1}$ selection as in Fig. 3. It shows that the relative enhancement of imbalanced dijet topologies seen in Figure 3 is due to the depletion in the absolute yield of balanced dijets—an observation valid also in the Pb+Pb measurement. The results in Figure 4 show a clear centrality evolution where the suppression of the balanced dijet yield gradually decreases from central to peripheral collisions.

To compare the x_j distribution between Xe+Xe and Pb+Pb in a different way, the x_j distributions are evaluated in intervals of the same event activity, quantified by ΣE_T^{FCal} . The choice of ΣE_T^{FCal} intervals matches those measured in Pb+Pb for centrality intervals 10–20%, 20–40%, and 40–60%. The corresponding centrality intervals in Xe+Xe collisions are given in Table II. The most central Pb+Pb interval (0–10%) cannot be used since the equivalent event activity is not present in Xe+Xe collisions. The Xe+Xe to

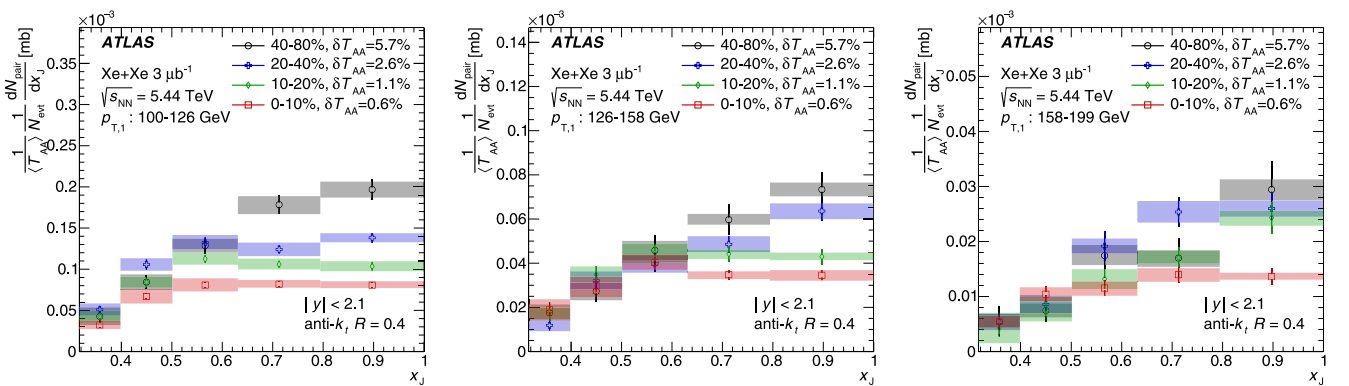


FIG. 4. Absolutely normalized x_j distribution evaluated in four centrality intervals and three p_T intervals of leading jet p_T : (left) $100 < p_{T,1} < 126$ GeV, (middle) $126 < p_{T,1} < 158$ GeV, and (right) $158 < p_{T,1} < 199$ GeV. Statistical and systematic uncertainties are represented by error bars and boxes, respectively. The δT_{AA} in the legend represents the relative uncertainty on $\langle T_{AA} \rangle$.

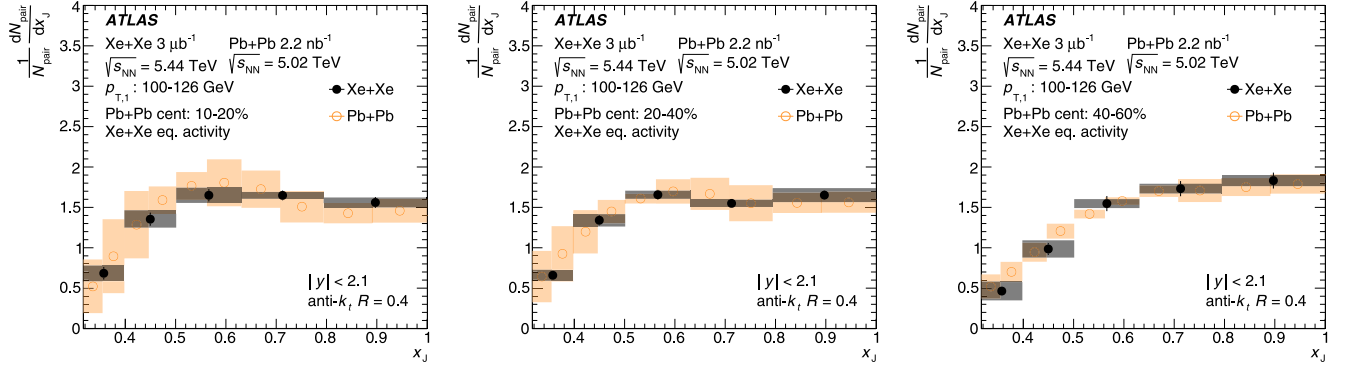


FIG. 5. Comparison of Xe+Xe (filled points) and Pb + Pb (open points) per-pair normalized x_j distributions in $100 < p_{T,1} < 126$ GeV and 10–20%, 20–40%, and 40–60% Pb + Pb centrality intervals and in the corresponding Xe+Xe ΣE_T^{Cal} intervals. Statistical and systematic uncertainties are represented by error bars and boxes, respectively.

Pb + Pb comparison of per-pair normalized x_j distributions is presented in Fig. 5 in the $100 < p_{T,1} < 126$ GeV interval. The distributions measured within the same event activity interval are consistent between Xe+Xe and Pb + Pb collisions. A similar agreement is also found in other $p_{T,1}$ selections. The smaller systematic uncertainties for the lower statistic Xe+Xe collisions are connected with the coarser binning used in

Xe+Xe data, which results in smaller bin-to-bin migrations and, consequently, smaller systematic uncertainties related to the unfolding procedure.

The comparison of absolutely normalized x_j distributions between Pb + Pb and Xe+Xe in the same event intervals is presented in the upper plots of Fig. 6. A clear difference between Xe+Xe and Pb + Pb distributions can be

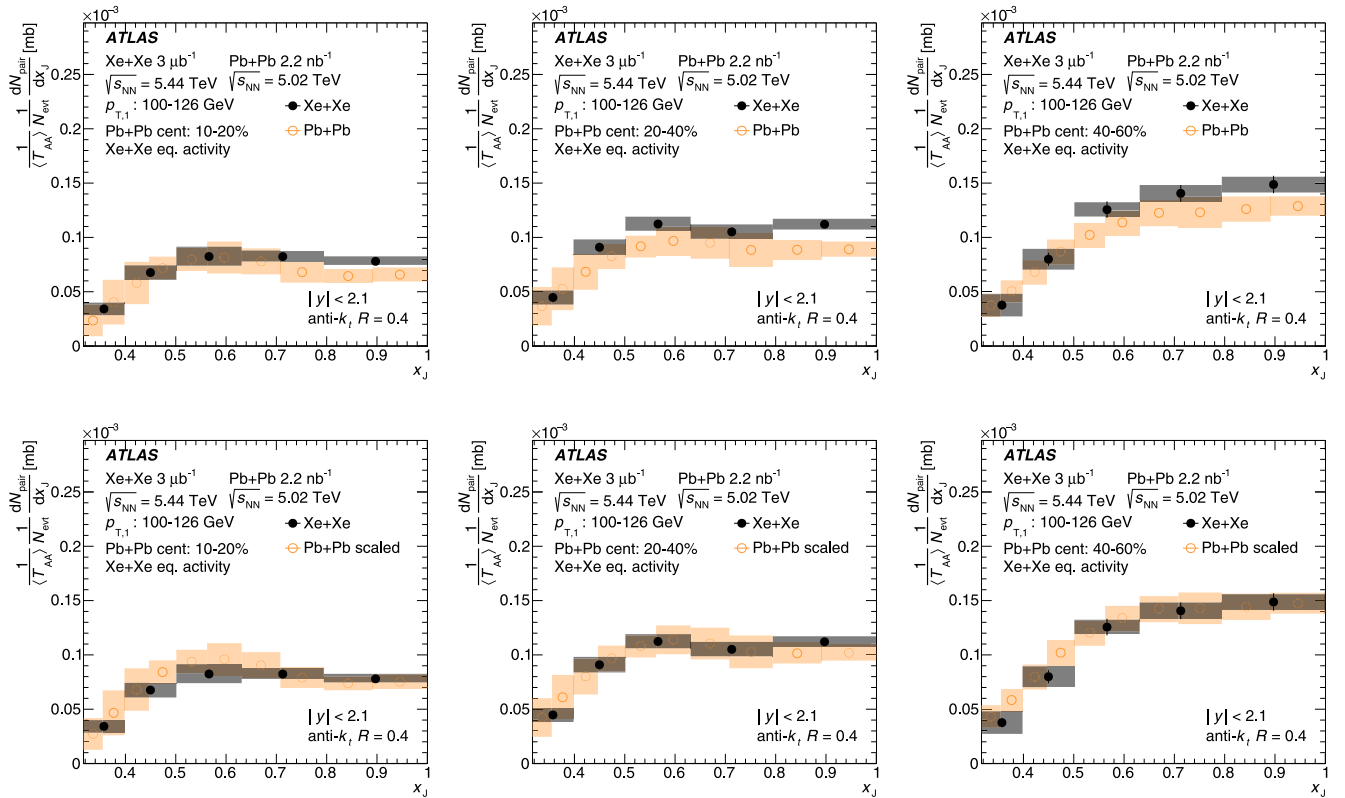


FIG. 6. Comparison of Xe+Xe (filled points) and Pb + Pb (open points) absolutely normalized x_j distributions in $100 < p_{T,1} < 126$ GeV and 10–20%, 20–40%, and 40–60% Pb + Pb centrality intervals and in the corresponding Xe+Xe ΣE_T^{Cal} intervals. The upper plots show directly measured distributions. The lower plots show the Pb + Pb distributions corrected for the impact of the difference between the center-of-mass energies of the hard scattering process in Xe+Xe and Pb + Pb collisions. Statistical and systematic uncertainties are represented by error bars and boxes, respectively.

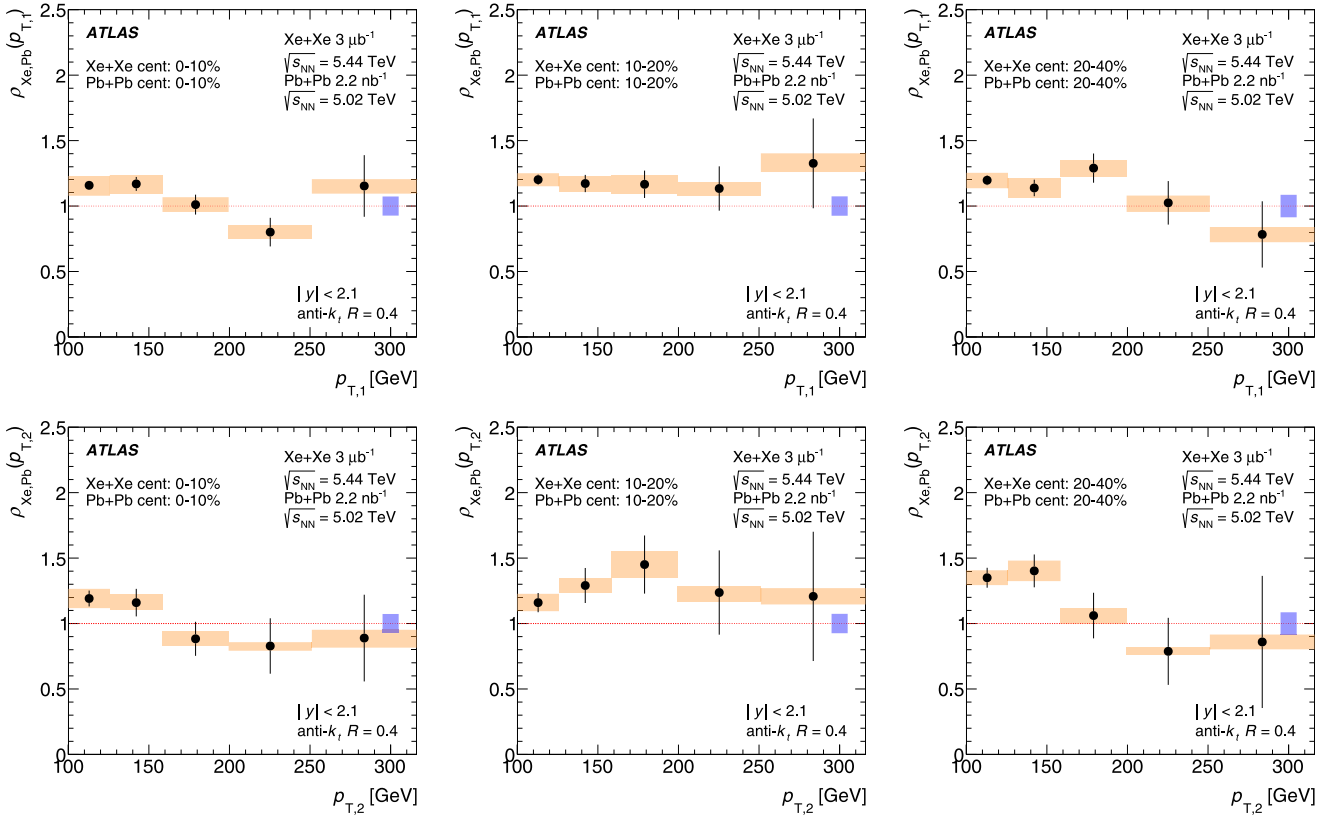


FIG. 7. The ratios of Xe+Xe and Pb+Pb pair nuclear-modification factors, $\rho_{\text{Xe,Pb}}$, evaluated as a function of (upper plots) $p_{T,1}$ and (lower plots) $p_{T,2}$ in the same centrality intervals. Statistical and systematic uncertainties are represented by error bars and boxes, respectively. The box centered at unity represents the fractional systematic uncertainty on $\langle T_{AA} \rangle$.

seen, with Xe+Xe having a larger absolute yield than Pb+Pb. This difference may be partially attributed to the difference between the hard process cross sections, due to the different center-of-mass energies of the initial hard scattering, in Xe+Xe and Pb+Pb collisions. To estimate the impact of the difference between the center-of-mass energies, the absolutely normalized x_j distributions in Pb+Pb collisions are scaled by $\mathcal{C}(x_j)$ defined in Eq. (3). The result is shown in the bottom plots of Fig. 6. After correcting for the difference between the center-of-mass energies of the initial hard scattering, the absolutely normalized x_j distributions agree between Xe+Xe and Pb+Pb collisions within uncertainties. The same conclusion is also found for other $p_{T,1}$ intervals. While the observed agreement could arise from canceling effects and large uncertainties, a natural explanation for this behavior is that the difference between the energies of the hard scattering process plays a significant role in the absolutely normalized x_j distributions.

In the case of per-pair normalized x_j distributions, the correction factor $\mathcal{C}(x_j)$ was found to be consistent with unity, which is consistent with observing an agreement of per-pair normalized x_j distributions between Xe+Xe and Pb+Pb collisions.

To characterize the differences between Xe+Xe and Pb+Pb dijet suppression in a more quantitative way, the Xe+Xe to Pb+Pb ratio of pair nuclear-modification factors,

$\rho_{\text{Xe,Pb}}$, are evaluated as defined in Sec. V. The $\rho_{\text{Xe,Pb}}(p_{T,1})$ and $\rho_{\text{Xe,Pb}}(p_{T,2})$ evaluated in the same Xe+Xe and Pb+Pb centrality intervals are shown in Fig. 7. The $\rho_{\text{Xe,Pb}}$ values obtained are systematically larger than unity, typically by 10% to 20% depending on centrality. Figure 8 shows $\rho_{\text{Xe,Pb}}$ evaluated in the same event activity intervals. In contrast to the centrality-based comparison, the $\rho_{\text{Xe,Pb}}$ values are consistent with unity within statistical and systematic uncertainties. This implies that the pair nuclear-modification factor in Xe+Xe collisions at $\sqrt{s_{NN}} = 5.44$ TeV is consistent with the same quantity measured at $\sqrt{s_{NN}} = 5.02$ TeV in Pb+Pb collisions, which suggests that the suppression of dijets does not differ in a significant way between Xe+Xe and Pb+Pb collisions when measured in the same event activity intervals.

Despite consistency of $\rho_{\text{Xe,Pb}}$ with the unity, we should still emphasize that any interpretation of the difference between the pair R_{AA} evaluated as a function of $p_{T,1}$ and $p_{T,2}$ as the difference between the overall suppression of leading and sub-leading jets needs to take into account that the yields entering the pair R_{AA} are conditional yields mutually dependent on kinematic selection criteria. Consequently, any interpretation of $\rho_{\text{Xe,Pb}}(p_{T,1})$, $\rho_{\text{Xe,Pb}}(p_{T,2})$ and $R_{AA}^{\text{pair}}(p_{T,1})$, $R_{AA}^{\text{pair}}(p_{T,2})$ must be performed in the context of theoretical model predictions that directly follow the dijet definition and projection procedures used in this analysis.

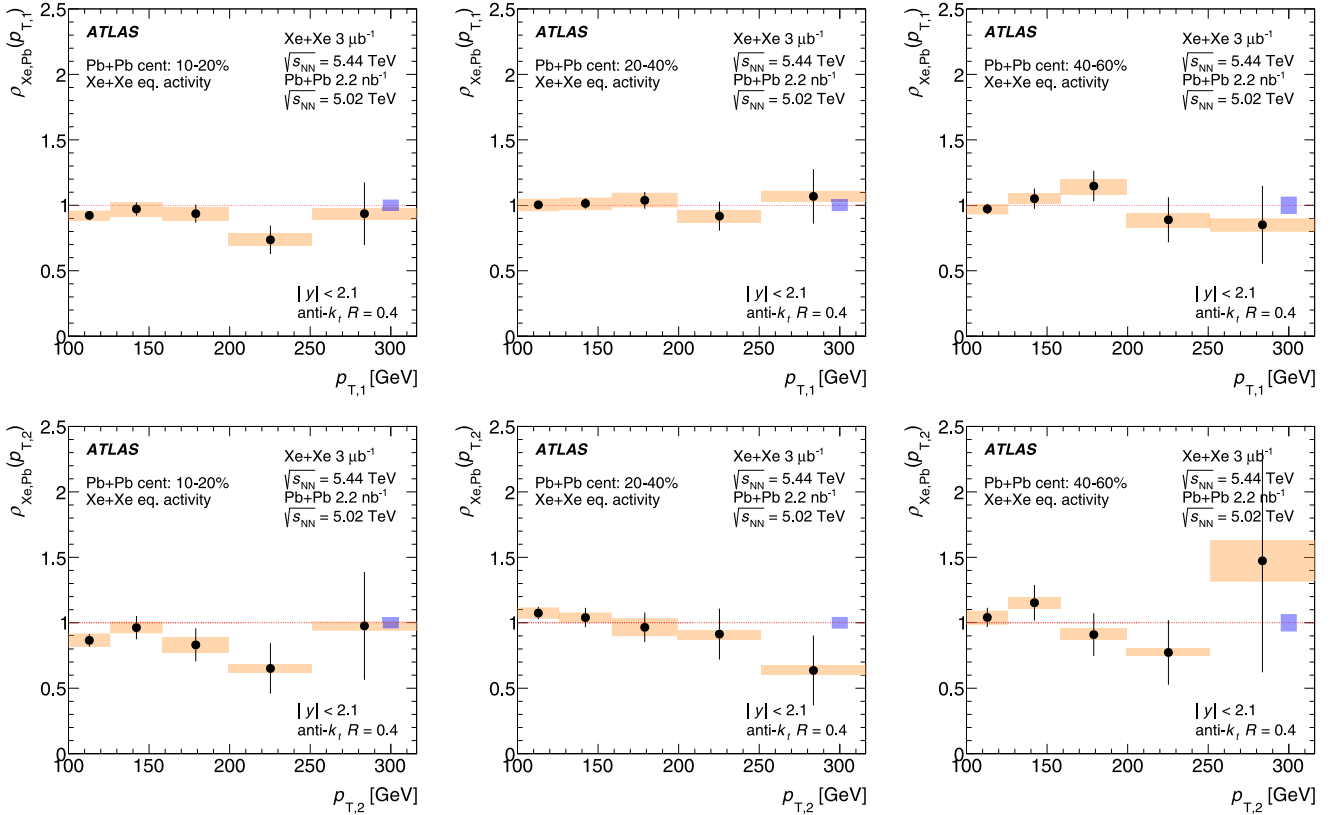


FIG. 8. The ratios of Xe+Xe and Pb+Pb pair nuclear-modification factors, $\rho_{\text{Xe,Pb}}$, evaluated as a function of (upper plots) $p_{T,1}$ and (lower plots) $p_{T,2}$ in the same ΣE_T^{FCal} intervals (selecting equivalent event activity). Statistical and systematic uncertainties are represented by error bars and boxes, respectively. The box centered at unity represents the fractional systematic uncertainty on $\langle T_{AA} \rangle$.

VIII. CONCLUSIONS

A measurement of per-pair normalized and absolutely normalized x_j distributions of dijets in Xe+Xe collisions at $\sqrt{s_{NN}} = 5.44$ TeV using $3 \mu\text{b}^{-1}$ of data collected with the ATLAS detector at the LHC is presented. The per-pair normalized x_j distributions indicate a higher relative rate of imbalanced dijets in central Xe+Xe collisions compared with peripheral ones. The absolutely normalized x_j distributions show that this feature arises predominantly from a depletion of the yields of more balanced dijets with x_j values close to unity.

The results are compared with a measurement of dijets in Pb+Pb collisions at $\sqrt{s_{NN}} = 5.02$ TeV by ATLAS. The x_j distributions are found to be consistent between Pb+Pb and Xe+Xe collisions when compared in the same event activity intervals and after correcting the absolutely normalized distributions for the expected difference between the hard process cross sections due to the different center-of-mass energies between Xe+Xe and Pb+Pb collisions. Furthermore, the differences between the dijet suppression in Xe+Xe and Pb+Pb are quantified by the ratio of pair nuclear-modification factors, $\rho_{\text{Xe,Pb}}$, which are found to be consistent with unity when evaluated in the same event activity intervals.

These results should provide input for a better understanding of the role of path length, energy density, and fluctuations in the jet-energy loss in the QGP and add a new input to

the quantification of its system size dependence. In particular, $\rho_{\text{Xe,Pb}}$ consistent with unity can be used for predicting the magnitude of jet quenching expected in future oxygen-oxygen collisions.

ACKNOWLEDGMENTS

We thank CERN for the very successful operation of the LHC, as well as the support staff from our institutions without whom ATLAS could not be operated efficiently. We acknowledge the support of ANPCyT, Argentina; YerPhI, Armenia; ARC, Australia; BMWFW and FWF, Austria; ANAS, Azerbaijan; CNPq and FAPESP, Brazil; NSERC, NRC, and CFI, Canada; CERN; ANID, Chile; CAS, MOST, and NSFC, China; Minciencias, Colombia; MEYS CR, Czech Republic; DNRF and DNSRC, Denmark; IN2P3-CNRS and CEA-DRF/IRFU, France; SRNSFG, Georgia; BMBF, HGF, and MPG, Germany; GSRI, Greece; RGC and Hong Kong SAR, China; ISF and Benozziyo Center, Israel; INFN, Italy; MEXT and JSPS, Japan; CNRST, Morocco; NWO, Netherlands; RCN, Norway; MEiN, Poland; FCT, Portugal; MNE/IFA, Romania; MESTD, Serbia; MSSR, Slovakia; ARRS and MIZŠ, Slovenia; DSI/NRF, South Africa; MICINN, Spain; SRC and Wallenberg Foundation, Sweden; SERI, SNSF, and Cantons of Bern and Geneva, Switzerland; MOST, Taiwan; TENMAK, Türkiye; STFC, United Kingdom; DOE and NSF,

United States of America. In addition, individual groups and members have received support from BCKDF, CANARIE, Compute Canada, and CRC, Canada; PRIMUS 21/SCI/017 and UNCE SCI/013, Czech Republic; COST, ERC, ERDF, Horizon 2020, and Marie Skłodowska-Curie Actions, European Union; Investissements d'Avenir Labex, Investissements d'Avenir Idex, and ANR, France; DFG and AvH Foundation, Germany; Herakleitos, Thales and Aristeia programs co-financed by EU-ESF and the Greek NSRF, Greece; BSF-NSF and MINERVA, Israel; Norwegian Financial Mechanism 2014-2021, Norway; NCN and NAWA, Poland; La Caixa Banking Foundation, CERCA Programme Generalitat de

Catalunya and PROMETEO and GenT Programmes Generalitat Valenciana, Spain; Göran Gustafssons Stiftelse, Sweden; The Royal Society and Leverhulme Trust, United Kingdom. The crucial computing support from all WLCG partners is acknowledged gratefully, in particular from CERN, the ATLAS Tier-1 facilities at TRIUMF (Canada), NDGF (Denmark, Norway, Sweden), CC-IN2P3 (France), KIT/GridKA (Germany), INFN-CNAF (Italy), NL-T1 (Netherlands), PIC (Spain), ASGC (Taiwan), RAL (UK), and BNL (USA), the Tier-2 facilities worldwide, and large non-WLCG resource providers. Major contributors of computing resources are listed in Ref. [49].

-
- [1] G.-Y. Qin and X.-N. Wang, Jet quenching in high-energy heavy-ion collisions, *Int. J. Mod. Phys. E* **24**, 1530014 (2015).
- [2] J.-P. Blaizot and Y. Mehtar-Tani, Jet structure in heavy ion collisions, *Int. J. Mod. Phys. E* **24**, 1530012 (2015).
- [3] L. Cunqueiro and A. M. Sickles, Studying the QGP with jets at the LHC and RHIC, *Prog. Part. Nucl. Phys.* **124**, 103940 (2022).
- [4] M. Aaboud *et al.* (ATLAS Collaboration), Measurement of the nuclear modification factor for inclusive jets in Pb + Pb collisions at $\sqrt{s_{NN}} = 5.02$ TeV with the ATLAS detector, *Phys. Lett. B* **790**, 108 (2019).
- [5] V. Khachatryan *et al.* (CMS Collaboration), Measurement of inclusive jet cross-sections in pp and PbPb collisions at $\sqrt{s_{NN}} = 2.76$ TeV, *Phys. Rev. C* **96**, 015202 (2017).
- [6] S. Acharya *et al.* (ALICE Collaboration), Measurements of inclusive jet spectra in pp and central Pb-Pb collisions at $\sqrt{s_{NN}} = 5.02$ TeV, *Phys. Rev. C* **101**, 034911 (2020).
- [7] G.-Y. Qin and B. Müller, Explanation of Dijet Asymmetry in Pb-Pb Collisions at the Large Hadron Collider, *Phys. Rev. Lett.* **106**, 162302 (2011); **108**, 189904(E) (2012).
- [8] J. G. Milhano and K. C. Zapp, Origins of the di-jet asymmetry in heavy ion collisions, *Eur. Phys. J. C* **76**, 288 (2016).
- [9] G. Aad *et al.* (ATLAS Collaboration), Observation of a Centrality-Dependent Dijet Asymmetry in Lead-Lead Collisions at $\sqrt{s_{NN}} = 2.76$ TeV with the ATLAS Detector at the LHC, *Phys. Rev. Lett.* **105**, 252303 (2010).
- [10] S. Chatrchyan *et al.* (CMS Collaboration), Observation and studies of jet quenching in PbPb collisions at $\sqrt{s_{NN}} = 2.76$ TeV, *Phys. Rev. C* **84**, 024906 (2011).
- [11] S. Chatrchyan *et al.* (CMS Collaboration), Jet momentum dependence of jet quenching in PbPb collisions at $\sqrt{s_{NN}} = 2.76$ TeV, *Phys. Lett. B* **712**, 176 (2012).
- [12] M. Aaboud *et al.* (ATLAS Collaboration), Measurement of jet p_T correlations in Pb + Pb and pp collisions at $\sqrt{s_{NN}} = 2.76$ TeV with the ATLAS detector, *Phys. Lett. B* **774**, 379 (2017).
- [13] G. Aad *et al.* (ATLAS Collaboration), Measurements of the suppression and correlations of dijets in Pb + Pb collisions at $\sqrt{s_{NN}} = 5.02$ TeV, *Phys. Rev. C* **107**, 054908 (2023).
- [14] G. Aad *et al.* (ATLAS Collaboration), Charged-hadron production in pp , p +Pb, Pb + Pb, and Xe+Xe collisions at $\sqrt{s_{NN}} = 5$ TeV with the ATLAS detector at the LHC, *J. High Energy Phys.* **07** (2023) 074.
- [15] A. M. Sirunyan *et al.* (CMS Collaboration), Charged-particle nuclear modification factors in XeXe collisions at $\sqrt{s_{NN}} = 5.44$ TeV, *J. High Energy Phys.* **10** (2018) 138.
- [16] S. Acharya *et al.* (ALICE Collaboration), Transverse momentum spectra and nuclear modification factors of charged particles in Xe-Xe collisions at $\sqrt{s_{NN}} = 5.44$ TeV, *Phys. Lett. B* **788**, 166 (2019).
- [17] Z. Citron *et al.*, Report from Working Group 5: Future physics opportunities for high-density QCD at the LHC with heavy-ion and proton beams, CERN Report No. CERN-LPCC-2018-07, 2019 (unpublished), <https://cds.cern.ch/record/2650176>
- [18] G. Aad *et al.* (ATLAS Collaboration), The ATLAS experiment at the CERN Large Hadron Collider, *JINST* **3**, S08003 (2008).
- [19] M. Aaboud *et al.* (ATLAS Collaboration), Performance of the ATLAS trigger system in 2015, *Eur. Phys. J. C* **77**, 317 (2017).
- [20] ATLAS Collaboration, The ATLAS Collaboration software and firmware, CERN Report No. ATL-SOFT-PUB-2021-001, 2021 (unpublished), <https://cds.cern.ch/record/2767187>
- [21] G. Aad *et al.* (ATLAS Collaboration), Jet energy measurement with the ATLAS detector in proton-proton collisions at $\sqrt{s} = 7$ TeV, *Eur. Phys. J. C* **73**, 2304 (2013).
- [22] C. Loizides, J. Kamin, and D. d'Enterria, Improved Monte Carlo Glauber predictions at present and future nuclear colliders, *Phys. Rev. C* **97**, 054910 (2018); **99**, 019901(E) (2019).
- [23] G. Aad *et al.* (ATLAS Collaboration), Measurement of the azimuthal anisotropy for charged particle production in $\sqrt{s_{NN}} = 2.76$ TeV lead-lead collisions with the ATLAS detector, *Phys. Rev. C* **86**, 014907 (2012).
- [24] G. Aad *et al.* (ATLAS Collaboration), Measurement of the pseudorapidity and transverse momentum dependence of the elliptic flow of charged particles in lead-lead collisions at $\sqrt{s_{NN}} = 2.76$ TeV with the ATLAS detector, *Phys. Lett. B* **707**, 330 (2012).
- [25] T. Sjöstrand, An introduction to PYTHIA 8.2, *Comput. Phys. Commun.* **191**, 159 (2015).
- [26] ATLAS Collaboration, ATLAS Pythia 8 tunes to 7 TeV data, CERN Report No. ATL-PHYS-PUB-2014-021, 2014 (unpublished), <https://cds.cern.ch/record/1966419>
- [27] R. D. Ball *et al.* (NNPDF Collaboration), Parton distributions with LHC data, *Nucl. Phys. B* **867**, 244 (2013).

- [28] S. Agostinelli *et al.*, GEANT4 – a simulation toolkit, *Nucl. Instrum. Methods Phys. Res., Sect. A* **506**, 250 (2003).
- [29] G. Aad *et al.* (ATLAS Collaboration), The ATLAS simulation infrastructure, *Eur. Phys. J. C* **70**, 823 (2010).
- [30] M. Bähr, Herwig++ physics and manual, *Eur. Phys. J. C* **58**, 639 (2008).
- [31] S. Gieseke, C. Rohr, and A. Siodmok, Colour reconnections in Herwig++, *Eur. Phys. J. C* **72**, 2225 (2012).
- [32] J. Pumplin *et al.*, New generation of parton distributions with uncertainties from global QCD analysis, *J. High Energy Phys.* **07** (2002) 012.
- [33] G. Aad *et al.* (ATLAS Collaboration), Measurements of azimuthal anisotropies of jet production in Pb + Pb collisions at $\sqrt{s_{NN}} = 5.02$ TeV with the ATLAS detector, *Phys. Rev. C* **105**, 064903 (2021).
- [34] M. Cacciari, G. P. Salam, and G. Soyez, The anti- k_t jet clustering algorithm, *J. High Energy Phys.* **04** (2008) 063.
- [35] M. Cacciari, G. P. Salam, and G. Soyez, FastJet user manual, *Eur. Phys. J. C* **72**, 1896 (2012).
- [36] M. Aaboud *et al.* (ATLAS Collaboration), Measurement of the azimuthal anisotropy of charged particles produced in $\sqrt{s_{NN}} = 5.02$ TeV Pb + Pb collisions with the ATLAS detector, *Eur. Phys. J. C* **78**, 997 (2018).
- [37] G. Aad *et al.* (ATLAS Collaboration), Jet energy measurement and its systematic uncertainty in proton–proton collisions at $\sqrt{s} = 7$ TeV with the ATLAS detector, *Eur. Phys. J. C* **75**, 17 (2015).
- [38] ATLAS Collaboration, Jet energy scale and its uncertainty for jets reconstructed using the ATLAS heavy ion jet algorithm, CERN Report No. ATLAS-CONF-2015-016, 2015 (unpublished), <https://cds.cern.ch/record/2008677>
- [39] M. Aaboud *et al.* (ATLAS Collaboration), Measurement of photon–jet transverse momentum correlations in 5.02 TeV Pb + Pb and pp collisions with ATLAS, *Phys. Lett. B* **789**, 167 (2019).
- [40] G. Aad *et al.* (ATLAS Collaboration), Measurement of the jet radius and transverse momentum dependence of inclusive jet suppression in lead–lead collisions at $\sqrt{s_{NN}} = 2.76$ TeV with the ATLAS detector, *Phys. Lett. B* **719**, 220 (2013).
- [41] T. Auye, Unfolding algorithms and tests using RooUnfold, in *2011 Workshop on Statistical Issues Related to Discovery Claims in Search Experiments and Unfolding (PHYSTAT 2011)*, Geneva January 17–20, 2011 (CERN, Geneva, 2011), p. 313, <https://cds.cern.ch/record/1306523>
- [42] G. D’Agostini, A multidimensional unfolding method based on Bayes’ theorem, *Nucl. Instrum. Methods Phys. Res., Sect. A* **362**, 487 (1995).
- [43] M. Aaboud *et al.* (ATLAS Collaboration), Jet energy scale measurements and their systematic uncertainties in proton–proton collisions at $\sqrt{s} = 13$ TeV with the ATLAS detector, *Phys. Rev. D* **96**, 072002 (2017).
- [44] G. Aad *et al.* (ATLAS Collaboration), Measurements of the Nuclear Modification Factor for Jets in Pb + Pb Collisions at $\sqrt{s_{NN}} = 2.76$ TeV with the ATLAS Detector, *Phys. Rev. Lett.* **114**, 072302 (2015).
- [45] M. Aaboud *et al.* (ATLAS Collaboration), Determination of jet calibration and energy resolution in proton–proton collisions at $\sqrt{s} = 8$ TeV using the ATLAS detector, *Eur. Phys. J. C* **80**, 1104 (2020).
- [46] G. Aad *et al.* (ATLAS Collaboration), Jet energy resolution in proton–proton collisions at $\sqrt{s} = 7$ TeV recorded in 2010 with the ATLAS detector, *Eur. Phys. J. C* **73**, 2306 (2013).
- [47] M. L. Miller, K. Reygers, S. J. Sanders, and P. Steinberg, Glauber modeling in high-energy nuclear collisions, *Annu. Rev. Nucl. Part. Sci.* **57**, 205 (2007).
- [48] D. d’Enterria and C. Loizides, Progress in the Glauber model at collider energies, *Annu. Rev. Nucl. Part. Sci.* **71**, 315 (2021).
- [49] ATLAS Collaboration, ATLAS computing acknowledgements, CERN Report No. ATL-SOFT-PUB-2021-003, 2021 (unpublished), <https://cds.cern.ch/record/2776662>

G. Aad¹⁰², B. Abbott¹²⁰, K. Abeling⁵⁵, S. H. Abidi²⁹, A. Abouhorma^{35e}, H. Abramowicz¹⁵¹, H. Abreu¹⁵⁰, Y. Abulaiti¹¹⁷, A. C. Abusleme Hoffman^{137a}, B. S. Acharya^{69a,69b,a}, C. Adam Bourdarios⁴, L. Adamczyk^{85a}, L. Adamek¹⁵⁵, S. V. Addepalli²⁶, J. Adelman¹¹⁵, A. Adiguzel^{21c}, S. Adorni⁵⁶, T. Auye¹³⁴, A. A. Affolder¹³⁶, Y. Afik³⁶, M. N. Agaras¹³, J. Agarwala^{73a,73b}, A. Aggarwal¹⁰⁰, C. Agheorghiesei^{27c}, J. A. Aguilar-Saavedra^{130f}, A. Ahmad³⁶, F. Ahmadov^{38,b}, W. S. Ahmed¹⁰⁴, S. Ahuja⁹⁵, X. Ai^{62a}, G. Aielli^{76a,76b}, M. Ait Tamlhat^{35e}, B. Aitbenchikh^{35a}, I. Aizenberg¹⁶⁹, M. Akbiyik¹⁰⁰, T. P. A. Åkesson⁹⁸, A. V. Akimov³⁷, D. Akiyama¹⁶⁸, N. N. Akolkar²⁴, K. Al Houry⁴¹, G. L. Alberghi^{23b}, J. Albert¹⁶⁵, P. Albicocco⁵³, S. Alderweireldt⁵², M. Aleksa³⁶, I. N. Aleksandrov³⁸, C. Alexa^{27b}, T. Alexopoulos¹⁰, A. Alfonsi¹¹⁴, F. Alfonsi^{23b}, M. Alhroob¹²⁰, B. Ali¹³², S. Ali¹⁴⁸, M. Aliev³⁷, G. Alimonti^{71a}, W. Alkahi⁵⁵, C. Allaire⁶⁶, B. M. M. Allbrooke¹⁴⁶, C. A. Allendes Flores^{137f}, P. P. Allport²⁰, A. Aloisio^{72a,72b}, F. Alonso⁹⁰, C. Alpigiani¹³⁸, M. Alvarez Estevez⁹⁹, A. Alvarez Fernandez¹⁰⁰, M. G. Alvigi^{72a,72b}, M. Aly¹⁰¹, Y. Amaral Coutinho^{82b}, A. Ambler¹⁰⁴, C. Amelung³⁶, M. Amerl¹⁰¹, C. G. Ames¹⁰⁹, D. Amidei¹⁰⁶, S. P. Amor Dos Santos^{130a}, K. R. Amos¹⁶³, V. Ananiev¹²⁵, C. Anastopoulos¹³⁹, T. Andeen¹¹, J. K. Anders³⁶, S. Y. Andreev^{47a,47b}, A. Andreatza^{71a,71b}, S. Angelidakis⁹, A. Angerami^{41,c}, A. V. Anisenkov³⁷, A. Annovi^{74a}, C. Antel⁵⁶, M. T. Anthony¹³⁹, E. Antipov¹⁴⁵, M. Antonelli⁵³, D. J. A. Antrim^{17a}, F. Anulli^{75a}, M. Aoki⁸³, T. Aoki¹⁵³, J. A. Aparisi Pozo¹⁶³, M. A. Aparo¹⁴⁶, L. Aperio Bella⁴⁸, C. Appelt¹⁸, N. Aranzabal³⁶, V. Araujo Ferraz^{82a}, C. Arcangeletti⁵³, A. T. H. Arce⁵¹, E. Arena⁹², J-F. Arguin¹⁰⁸, S. Argyropoulos⁵⁴, J.-H. Arling⁴⁸, A. J. Armbruster³⁶, O. Arnaez⁴, H. Arnold¹¹⁴, Z. P. Arrubarrena Tame¹⁰⁹, G. Artoni^{75a,75b}, H. Asada¹¹¹, K. Asai¹¹⁸, S. Asai¹⁵³, N. A. Asbah⁶¹, J. Assahsah^{35d}, K. Assamagan²⁹, R. Astalos^{28a}, R. J. Atkin^{33a}, M. Atkinson¹⁶², N. B. Atlay¹⁸, H. Atmani^{62b}, P. A. Atmasiddha¹⁰⁶, K. Augsten¹³², S. Auricchio^{72a,72b}, A. D. Auriol²⁰, V. A. Austrup¹⁷¹, G. Avner¹⁵⁰, G. Avolio³⁶, K. Axiotis⁵⁶, G. Azuelos^{108,d}

- D. Babal ^{28b} H. Bachacou ¹³⁵ K. Bachas ^{152,e} A. Bachiu ³⁴ F. Backman ^{47a,47b} A. Badea ⁶¹ P. Bagnaia ^{75a,75b}
M. Bahmani ¹⁸ A. J. Bailey ¹⁶³ V. R. Bailey ¹⁶² J. T. Baines ¹³⁴ C. Bakalis ¹⁰ O. K. Baker ¹⁷² E. Bakos ¹⁵
D. Bakshi Gupta ⁸ R. Balasubramanian ¹¹⁴ E. M. Baldin ³⁷ P. Balek ^{85a} E. Ballabene ^{71a,71b} F. Balli ¹³⁵
L. M. Balmes ^{63a} W. K. Balunas ³² J. Balz ¹⁰⁰ E. Banas ⁸⁶ M. Bandieramonte ¹²⁹ A. Bandyopadhyay ²⁴
S. Bansal ²⁴ L. Barak ¹⁵¹ E. L. Barberio ¹⁰⁵ D. Barberis ^{57b,57a} M. Barbero ¹⁰² G. Barbour ⁹⁶ K. N. Barends ^{33a}
T. Barillari ¹¹⁰ M-S. Barisits ³⁶ T. Barklow ¹⁴³ P. Baron ¹²² D. A. Baron Moreno ¹⁰¹ A. Baroncelli ^{62a}
G. Barone ²⁹ A. J. Barr ¹²⁶ L. Barranco Navarro ^{47a,47b} F. Barreiro ⁹⁹ J. Barreiro Guimarães da Costa ^{14a}
U. Barron ¹⁵¹ M. G. Barros Teixeira ^{130a} S. Barsov ³⁷ F. Bartels ^{63a} R. Bartoldus ¹⁴³ A. E. Barton ⁹¹ P. Bartos ^{28a}
A. Basan ¹⁰⁰ M. Baselga ⁴⁹ A. Bassalat ^{66,f} M. J. Basso ¹⁵⁵ C. R. Basson ¹⁰¹ R. L. Bates ⁵⁹ S. Batlamous ^{35e}
J. R. Batley ³² B. Batool ¹⁴¹ M. Battaglia ¹³⁶ D. Battulga ¹⁸ M. Bauce ^{75a,75b} M. Bauer ³⁶ P. Bauer ²⁴
J. B. Beacham ⁵¹ T. Beau ¹²⁷ P. H. Beauchemin ¹⁵⁸ F. Becherer ⁵⁴ P. Bechtle ²⁴ H. P. Beck ^{19,g} K. Becker ¹⁶⁷
A. J. Beddall ^{21d} V. A. Bednyakov ³⁸ C. P. Bee ¹⁴⁵ L. J. Beemster ¹⁵ T. A. Beermann ³⁶ M. Begalli ^{82d} M. Begel ²⁹
A. Behera ¹⁴⁵ J. K. Behr ⁴⁸ J. F. Beirer ⁵⁵ F. Beisiegel ²⁴ M. Belfkir ¹⁵⁹ G. Bella ¹⁵¹ L. Bellagamba ^{23b}
A. Bellerive ³⁴ P. Bellos ²⁰ K. Beloborodov ³⁷ N. L. Belyaev ³⁷ D. Benckekroun ^{35a} F. Bendebba ^{35a}
Y. Benhammou ¹⁵¹ M. Benoit ²⁹ J. R. Bensinger ²⁶ S. Bentvelsen ¹¹⁴ L. Beresford ⁴⁸ M. Beretta ⁵³
E. Bergeaas Kuutmann ¹⁶¹ N. Berger ⁴ B. Bergmann ¹³² J. Beringer ^{17a} S. Berlendis ⁷ G. Bernardi ⁵
C. Bernius ¹⁴³ F. U. Bernlochner ²⁴ T. Berry ⁹⁵ P. Berta ¹³³ A. Berthold ⁵⁰ I. A. Bertram ⁹¹ S. Bethke ¹¹⁰
A. Betti ^{75a,75b} A. J. Bevan ⁹⁴ M. Bhamjee ^{33c} S. Bhatta ¹⁴⁵ D. S. Bhattacharya ¹⁶⁶ P. Bhattacharai ²⁶
V. S. Bhopatkar ¹²¹ R. Bi ^{29,h} R. M. Bianchi ¹²⁹ G. Bianco ^{23b,23a} O. Biebel ¹⁰⁹ R. Bielski ¹²³ M. Biglietti ^{77a}
T. R. V. Billoud ¹³² M. Bindi ⁵⁵ A. Bingul ^{21b} C. Bini ^{75a,75b} A. Biondini ⁹² C. J. Birch-sykes ¹⁰¹ G. A. Bird ^{20,134}
M. Birman ¹⁶⁹ M. Biros ¹³³ T. Bisanz ³⁶ E. Bisceglie ^{43b,43a} D. Biswas ¹⁷⁰ A. Bitadze ¹⁰¹ K. Björke ¹²⁵
I. Bloch ⁴⁸ C. Blocker ²⁶ A. Blue ⁵⁹ U. Blumenschein ⁹⁴ J. Blumenthal ¹⁰⁰ G. J. Bobbink ¹¹⁴ V. S. Bobrovnikov ³⁷
M. Boehler ⁵⁴ B. Boehm ¹⁶⁶ D. Bogavac ³⁶ A. G. Bogdanichikov ³⁷ C. Bohm ^{47a} V. Boisvert ⁹⁵ P. Bokan ⁴⁸
T. Bold ^{85a} M. Bomben ⁵ M. Bona ⁹⁴ M. Boonekamp ¹³⁵ C. D. Booth ⁹⁵ A. G. Borbély ⁵⁹ I. S. Bordulev ³⁷
H. M. Borecka-Bielska ¹⁰⁸ L. S. Borgna ⁹⁶ G. Borissov ⁹¹ D. Bortoletto ¹²⁶ D. Boscherini ^{23b} M. Bosman ¹³
J. D. Bossio Sola ³⁶ K. Bouaouda ^{35a} N. Bouchhar ¹⁶³ J. Boudreau ¹²⁹ E. V. Bouhova-Thacker ⁹¹ D. Boumediene ⁴⁰
R. Bouquet ⁵ A. Boveia ¹¹⁹ J. Boyd ³⁶ D. Boye ²⁹ I. R. Boyko ³⁸ J. Bracinik ²⁰ N. Brahimi ^{62d} G. Brandt ¹⁷¹
O. Brandt ³² F. Braren ⁴⁸ B. Brau ¹⁰³ J. E. Brau ¹²³ R. Brener ¹⁶⁹ L. Brenner ¹¹⁴ R. Brenner ¹⁶¹ S. Bressler ¹⁶⁹
D. Britton ⁵⁹ D. Britzger ¹¹⁰ I. Brock ²⁴ G. Brooijmans ⁴¹ W. K. Brooks ^{137f} E. Brost ²⁹ L. M. Brown ¹⁶⁵
T. L. Bruckler ¹²⁶ P. A. Bruckman de Renstrom ⁸⁶ B. Brüers ⁴⁸ D. Bruncko ^{28b,i} A. Bruni ^{23b} G. Bruni ^{23b}
M. Bruschi ^{23b} N. Bruscino ^{75a,75b} T. Buanes ¹⁶ Q. Buat ¹³⁸ A. G. Buckley ⁵⁹ I. A. Budagov ^{38,i} M. K. Bugge ¹²⁵
O. Bulekov ³⁷ B. A. Bullard ¹⁴³ S. Burdin ⁹² C. D. Burgard ⁴⁹ A. M. Burger ⁴⁰ B. Burghgrave ⁸ O. Burlayenko ⁵⁴
J. T. P. Burr ³² C. D. Burton ¹¹ J. C. Burzynski ¹⁴² E. L. Busch ⁴¹ V. Büscher ¹⁰⁰ P. J. Bussey ⁵⁹ J. M. Butler ²⁵
C. M. Buttar ⁵⁹ J. M. Butterworth ⁹⁶ W. Buttinger ¹³⁴ C. J. Buxo Vazquez ¹⁰⁷ A. R. Buzykaev ³⁷ G. Cabras ^{23b}
S. Cabrera Urbán ¹⁶³ D. Caforio ⁵⁸ H. Cai ¹²⁹ Y. Cai ^{14a,14e} V. M. M. Cairo ³⁶ O. Cakir ^{3a} N. Calace ³⁶
P. Calafiura ^{17a} G. Calderini ¹²⁷ P. Calfayan ⁶⁸ G. Callea ⁵⁹ L. P. Caloba ^{82b} D. Calvet ⁴⁰ S. Calvet ⁴⁰
T. P. Calvet ¹⁰² M. Calvetti ^{74a,74b} R. Camacho Toro ¹²⁷ S. Camarda ³⁶ D. Camarero Munoz ²⁶ P. Camarri ^{76a,76b}
M. T. Camerlingo ^{72a,72b} D. Cameron ¹²⁵ C. Camincher ¹⁶⁵ M. Campanelli ⁹⁶ A. Camplani ⁴² V. Canale ^{72a,72b}
A. Canesse ¹⁰⁴ M. Cano Bret ⁸⁰ J. Cantero ¹⁶³ Y. Cao ¹⁶² F. Capocasa ²⁶ M. Capua ^{43b,43a} A. Carbone ^{71a,71b}
R. Cardarelli ^{76a} J. C. J. Cardenas ⁸ F. Cardillo ¹⁶³ T. Carli ³⁶ G. Carlino ^{72a} J. I. Carlotto ¹³ B. T. Carlson ^{129,j}
E. M. Carlson ^{165,156a} L. Carminati ^{71a,71b} M. Carnesale ^{75a,75b} S. Caron ¹¹³ E. Carquin ^{137f} S. Carrá ^{71a,71b}
G. Carratta ^{23b,23a} F. Carrio Argos ^{33g} J. W. S. Carter ¹⁵⁵ T. M. Carter ⁵² M. P. Casado ^{13,k} A. F. Casha ¹⁵⁵
M. Caspar ⁴⁸ E. G. Castiglia ¹⁷² F. L. Castillo ^{63a} L. Castillo Garcia ¹³ V. Castillo Gimenez ¹⁶³ N. F. Castro ^{130a,130e}
A. Catinaccio ³⁶ J. R. Catmore ¹²⁵ V. Cavaliere ²⁹ N. Cavalli ^{23b,23a} V. Cavasinni ^{74a,74b} Y. C. Cekmecelioglu ⁴⁸
E. Celebi ^{21a} F. Celli ¹²⁶ M. S. Centonze ^{70a,70b} K. Cerny ¹²² A. S. Cerqueira ^{82a} A. Cerri ¹⁴⁶ L. Cerrito ^{76a,76b}
F. Cerutti ^{17a} B. Cervato ¹⁴¹ A. Cervelli ^{23b} G. Cesarini ⁵³ S. A. Cetin ^{21d} Z. Chadi ^{35a} D. Chakraborty ¹¹⁵
M. Chala ^{130f} J. Chan ¹⁷⁰ W. Y. Chan ¹⁵³ J. D. Chapman ³² B. Chargeishvili ^{149b} D. G. Charlton ²⁰
T. P. Charman ⁹⁴ M. Chatterjee ¹⁹ C. Chauhan ¹³³ S. Chekanov ⁶ S. V. Chekulaev ^{156a} G. A. Chelkov ^{38,1}
A. Chen ¹⁰⁶ B. Chen ¹⁵¹ B. Chen ¹⁶⁵ H. Chen ^{14c} H. Chen ²⁹ J. Chen ^{62c} J. Chen ¹⁴² S. Chen ¹⁵³ S. J. Chen ^{14c}
X. Chen ^{62c} X. Chen ^{14b,m} Y. Chen ^{62a} C. L. Cheng ¹⁷⁰ H. C. Cheng ^{64a} S. Cheong ¹⁴³ A. Cheplakov ³⁸
E. Chermushkina ⁴⁸ E. Cherepanova ¹¹⁴ R. Cherkaoui El Moursli ^{35e} E. Cheu ⁷ K. Cheung ⁶⁵ L. Chevalier ¹³⁵
V. Chiarella ⁵³ G. Chiarelli ^{74a} N. Chiedde ¹⁰² G. Chiodini ^{70a} A. S. Chisholm ²⁰ A. Chitan ^{27b} M. Chitishvili ¹⁶³
M. V. Chizhov ³⁸ K. Choi ¹¹ A. R. Chomont ^{75a,75b} Y. Chou ¹⁰³ E. Y. S. Chow ¹¹⁴ T. Chowdhury ^{33g}
L. D. Christopher ^{33g} K. L. Chu ¹⁶⁹ M. C. Chu ^{64a} X. Chu ^{14a,14e} J. Chudoba ¹³¹ J. J. Chwastowski ⁸⁶ D. Cieri ¹¹⁰
K. M. Ciesla ^{85a} V. Cindro ⁹³ A. Ciocio ^{17a} F. Ciotto ^{72a,72b} Z. H. Citron ^{169,n} M. Citterio ^{71a} D. A. Ciubotaru ^{27b}
B. M. Ciungu ¹⁵⁵ A. Clark ⁵⁶ P. J. Clark ⁵² J. M. Clavijo Columbie ⁴⁸ S. E. Clawson ¹⁰¹ C. Clement ^{47a,47b}
J. Clercx ⁴⁸ L. Clissa ^{23b,23a} Y. Coadou ¹⁰² M. Cobal ^{69a,69c} A. Coccaro ^{57b} R. F. Coelho Barrue ^{130a}
R. Coelho Lopes De Sa ¹⁰³ S. Coelli ^{71a} H. Cohen ¹⁵¹ A. E. C. Coimbra ^{71a,71b} B. Cole ⁴¹ J. Collot ⁶⁰

- P. Conde Muiño ^{130a,130g} M. P. Connell ^{33c} S. H. Connell ^{33c} I. A. Connelly ⁵⁹ E. I. Conroy ¹²⁶ F. Conventi ^{72a,o}
H. G. Cooke ²⁰ A. M. Cooper-Sarkar ¹²⁶ F. Cormier ¹⁶⁴ L. D. Corpe ³⁶ M. Corradi ^{75a,75b} F. Corriveau ^{104,p}
A. Cortes-Gonzalez ¹⁸ M. J. Costa ¹⁶³ F. Costanza ⁴ D. Costanzo ¹³⁹ B. M. Cote ¹¹⁹ G. Cowan ⁹⁵ K. Cranmer ¹¹⁷
D. Cremonini ^{23b,23a} S. Crépé-Renaudin ⁶⁰ F. Crescioli ¹²⁷ M. Cristinziani ¹⁴¹ M. Cristoforetti ^{78a,78b,q} V. Croft ¹¹⁴
J. E. Crosby ¹²¹ G. Crosetti ^{43b,43a} A. Cueto ³⁶ T. Cuhadar Donszelmann ¹⁶⁰ H. Cui ^{14a,14e} Z. Cui ⁷
W. R. Cunningham ⁵⁹ F. Curcio ^{43b,43a} P. Czodrowski ³⁶ M. M. Czurylo ^{63b} M. J. Da Cunha Sargedas De Sousa ^{62a}
J. V. Da Fonseca Pinto ^{82b} C. Da Via ¹⁰¹ W. Dabrowski ^{85a} T. Dado ⁴⁹ S. Dahbi ^{33g} T. Dai ¹⁰⁶ C. Dallapiccola ¹⁰³
M. Dam ⁴² G. D'amen ²⁹ V. D'Amico ¹⁰⁹ J. Damp ¹⁰⁰ J. R. Dandoy ¹²⁸ M. F. Daneri ³⁰ M. Danninger ¹⁴²
V. Dao ³⁶ G. Darbo ^{57b} S. Darmora ⁶ S. J. Das ^{29,h} S. D'Auria ^{71a,71b} C. David ^{156b} T. Davidek ¹³³
B. Davis-Purcell ³⁴ I. Dawson ⁹⁴ K. De ⁸ R. De Asmundis ^{72a} N. De Biase ⁴⁸ S. De Castro ^{23b,23a} N. De Groot ¹¹³
P. de Jong ¹¹⁴ H. De la Torre ¹⁰⁷ A. De Maria ^{14c} A. De Salvo ^{75a} U. De Sanctis ^{76a,76b} A. De Santo ¹⁴⁶
J. B. De Vivie De Regie ⁶⁰ D. V. Dedovich ³⁸ J. Degens ¹¹⁴ A. M. Deiana ⁴⁴ F. Del Corso ^{23b,23a} J. Del Peso ⁹⁹
F. Del Rio ^{63a} F. Deliot ¹³⁵ C. M. Delitzsch ⁴⁹ M. Della Pietra ^{72a,72b} D. Della Volpe ⁵⁶ A. Dell'Acqua ³⁶
L. Dell'Asta ^{71a,71b} M. Delmastro ⁴ P. A. Delsart ⁶⁰ S. Demers ¹⁷² M. Demichev ³⁸ S. P. Denisov ³⁷
L. D'ErAMO ¹¹⁵ D. Derendarz ⁸⁶ F. Derue ¹²⁷ P. Dervan ⁹² K. Desch ²⁴ K. Dette ¹⁵⁵ C. Deutsch ²⁴
F. A. Di Bello ^{57b,57a} A. Di Ciaccio ^{76a,76b} L. Di Ciaccio ⁴ A. Di Domenico ^{75a,75b} C. Di Donato ^{72a,72b}
A. Di Girolamo ³⁶ G. Di Gregorio ⁵ A. Di Luca ^{78a,78b} B. Di Micco ^{77a,77b} R. Di Nardo ^{77a,77b} C. Diaconu ¹⁰²
F. A. Dias ¹¹⁴ T. Dias Do Vale ¹⁴² M. A. Diaz ^{137a,137b} F. G. Diaz Capriles ²⁴ M. Didenko ¹⁶³ E. B. Diehl ¹⁰⁶
L. Diehl ⁵⁴ S. Díez Cornell ⁴⁸ C. Díez Pardos ¹⁴¹ C. Dimitriadi ^{24,161} A. Dimitrievska ^{17a} J. Dingfelder ²⁴
I-M. Dinu ^{27b} S. J. Dittmeier ^{63b} F. Dittus ³⁶ F. Djama ¹⁰² T. Djobava ^{149b} J. I. Djuvsland ¹⁶ C. Doglioni ^{101,98}
J. Dolejsi ¹³³ Z. Dolezal ¹³³ M. Donadelli ^{82c} B. Dong ¹⁰⁷ J. Donini ⁴⁰ A. D'Onofrio ^{77a,77b} M. D'Onofrio ⁹²
J. Dopke ¹³⁴ A. Doria ^{72a} M. T. Dova ⁹⁰ A. T. Doyle ⁵⁹ M. A. Draguet ¹²⁶ E. Drechsler ¹⁴² E. Dreyer ¹⁶⁹
I. Drivas-koulouris ¹⁰ A. S. Drobac ¹⁵⁸ M. Drozdova ⁵⁶ D. Du ^{62a} T. A. du Pree ¹¹⁴ F. Dubinin ³⁷ M. Dubovsky ^{28a}
E. Duchovni ¹⁶⁹ G. Duckeck ¹⁰⁹ O. A. Ducu ^{27b} D. Duda ¹¹⁰ A. Dudarev ³⁶ E. R. Duden ²⁶ M. D'uffizi ¹⁰¹
L. Duflo ⁶⁶ M. Dührssen ³⁶ C. Dülsen ¹⁷¹ A. E. Dumitriu ^{27b} M. Dunford ^{63a} S. Dungs ⁴⁹ K. Dunne ^{47a,47b}
A. Duperrin ¹⁰² H. Duran Yildiz ^{3a} M. Düren ⁵⁸ A. Durglishvili ^{149b} B. L. Dwyer ¹¹⁵ G. I. Dyckes ^{17a}
M. Dyndal ^{85a} S. Dysch ¹⁰¹ B. S. Dziedzic ⁸⁶ Z. O. Earnshaw ¹⁴⁶ G. H. Eberwein ¹²⁶ B. Eckerova ^{28a}
S. Eggebrecht ⁵⁵ M. G. Eggleston ⁵¹ E. Egidio Purcino De Souza ¹²⁷ L. F. Ehrke ⁵⁶ G. Eigen ¹⁶ K. Einsweiler ^{17a}
T. Ekelof ¹⁶¹ P. A. Ekman ⁹⁸ Y. El Ghazali ^{35b} H. El Jarrari ^{35e,148} A. El Moussaouy ^{35a} V. Ellajosyula ¹⁶¹
M. Ellert ¹⁶¹ F. Ellinghaus ¹⁷¹ A. A. Elliot ⁹⁴ N. Ellis ³⁶ J. Elmsheuser ²⁹ M. Elsing ³⁶ D. Emelianov ¹³⁴
Y. Enari ¹⁵³ I. Ene ^{17a} S. Epari ¹³ J. Erdmann ⁴⁹ P. A. Erland ⁸⁶ M. Errenst ¹⁷¹ M. Escalier ⁶⁶ C. Escobar ¹⁶³
E. Etzion ¹⁵¹ G. Evans ^{130a} H. Evans ⁶⁸ L. S. Evans ⁹⁵ M. O. Evans ¹⁴⁶ A. Ezhilov ³⁷ S. Ezzarqtouni ^{35a}
F. Fabbri ⁵⁹ L. Fabbri ^{23b,23a} G. Facini ⁹⁶ V. Fadeyev ¹³⁶ R. M. Fakhrudinov ³⁷ S. Falciano ^{75a}
L. F. Falda Ulhoa Coelho ³⁶ P. J. Falke ²⁴ J. Faltova ¹³³ C. Fan ¹⁶² Y. Fan ^{14a} Y. Fang ^{14a,14e} M. Fanti ^{71a,71b}
M. Faraj ^{69a,69b} Z. Farazpay ⁹⁷ A. Farbin ⁸ A. Farilla ^{77a} T. Farooque ¹⁰⁷ S. M. Farrington ⁵² F. Fassi ^{35e}
D. Fassouliotis ⁹ M. Faucci Giannelli ^{76a,76b} W. J. Fawcett ³² L. Fayard ⁶⁶ P. Federic ¹³³ P. Federicova ¹³¹
O. L. Fedin ^{37,1} G. Fedotov ³⁷ M. Feickert ¹⁷⁰ L. Feligioni ¹⁰² A. Fell ¹³⁹ D. E. Fellers ¹²³ C. Feng ^{62b}
M. Feng ^{14b} Z. Feng ¹¹⁴ M. J. Fenton ¹⁶⁰ A. B. Fenyuk ³⁷ L. Ferencz ⁴⁸ R. A. M. Ferguson ⁹¹
S. I. Fernandez Luengo ^{137f} M. J. V. Fernoux ¹⁰² J. Ferrando ⁴⁸ A. Ferrari ¹⁶¹ P. Ferrari ^{114,113} R. Ferrari ^{73a}
D. Ferrere ⁵⁶ C. Ferretti ¹⁰⁶ F. Fiedler ¹⁰⁰ A. Filipčić ¹⁰⁰ E. K. Filmer ¹ F. Filthaut ¹¹³ M. C. N. Fiolhais ^{130a,130c,r}
L. Fiorini ¹⁶³ W. C. Fisher ¹⁰⁷ T. Fitschen ¹⁰¹ P. M. Fitzhugh ¹³⁵ I. Fleck ¹⁴¹ P. Fleischmann ¹⁰⁶ T. Flick ¹⁷¹
L. Flores ¹²⁸ M. Flores ^{33d,33e,33f,s} L. R. Flores Castillo ^{64a} F. M. Follega ^{78a,78b} N. Fomin ¹⁶ J. H. Foo ¹⁵⁵
B. C. Forland ⁶⁸ A. Formica ¹³⁵ A. C. Forti ¹⁰¹ E. Fortin ³⁶ A. W. Fortman ⁶¹ M. G. Foti ^{17a} L. Fountas ^{9,t}
D. Fournier ⁶⁶ H. Fox ⁹¹ P. Francavilla ^{74a,74b} S. Francescato ⁶¹ S. Franchellucci ⁵⁶ M. Franchini ^{23b,23a}
S. Franchino ^{63a} D. Francis ³⁶ L. Franco ¹¹³ L. Franconi ⁴⁸ M. Franklin ⁶¹ G. Frattari ²⁶ A. C. Freegard ⁹⁴
W. S. Freund ^{82b} Y. Y. Frid ¹⁵¹ N. Fritzsche ⁵⁰ A. Froch ⁵⁴ D. Froidevaux ³⁶ J. A. Frost ¹²⁶ Y. Fu ^{62a}
M. Fujimoto ¹¹⁸ E. Fullana Torregrosa ^{163,i} E. Furtado De Simas Filho ^{82b} J. Fuster ¹⁶³ A. Gabrielli ^{23b,23a}
A. Gabrielli ¹⁵⁵ P. Gadow ⁴⁸ G. Gagliardi ^{57b,57a} L. G. Gagnon ^{17a} E. J. Gallas ¹²⁶ B. J. Gallop ¹³⁴ K. K. Gan ¹¹⁹
S. Ganguly ¹⁵³ J. Gao ^{62a} Y. Gao ⁵² F. M. Garay Walls ^{137a,137b} B. Garcia ^{29,h} C. García ¹⁶³ A. Garcia Alonso ¹¹⁴
A. G. Garcia Caffaro ¹⁷² J. E. García Navarro ¹⁶³ M. Garcia-Sciveres ^{17a} R. W. Gardner ³⁹ D. Garg ⁸⁰
R. B. Garg ^{143,u} C. A. Garner ¹⁵⁵ S. J. Gasiorowski ¹³⁸ P. Gaspar ^{82b} G. Gaudio ^{73a} V. Gautam ¹³ P. Gauzzi ^{75a,75b}
I. L. Gavrilenko ³⁷ A. Gavriluk ³⁷ C. Gay ¹⁶⁴ G. Gaycken ⁴⁸ E. N. Gazis ¹⁰ A. A. Geanta ^{27b,27e} C. M. Gee ¹³⁶
C. Gemme ^{57b} M. H. Genest ⁶⁰ S. Gentile ^{75a,75b} S. George ⁹⁵ W. F. George ²⁰ T. Gerialis ⁴⁶ L. O. Gerlach ⁵⁵
P. Gessinger-Befurt ³⁶ M. E. Geyik ¹⁷¹ M. Ghneimat ¹⁴¹ K. Ghorbanian ⁹⁴ A. Ghosal ¹⁴¹ A. Ghosh ¹⁶⁰ A. Ghosh ⁷
B. Giacobbe ^{23b} S. Giagu ^{75a,75b} P. Giannetti ^{74a} A. Giannini ^{62a} S. M. Gibson ⁹⁵ M. Gignac ¹³⁶ D. T. Gil ^{85b}
A. K. Gilbert ^{85a} B. J. Gilbert ⁴¹ D. Gillberg ³⁴ G. Gilles ¹¹⁴ N. E. K. Gillwald ⁴⁸ L. Ginabat ¹²⁷
D. M. Gingrich ^{2,d} M. P. Giordani ^{69a,69c} P. F. Giraud ¹³⁵ G. Giugliarelli ^{69a,69c} D. Giugni ^{71a} F. Giuli ³⁶
I. Gkialas ^{9,t} L. K. Gladilin ³⁷ C. Glasman ⁹⁹ G. R. Gledhill ¹²³ M. Glisic ¹²³ I. Gnesi ^{43b,v} Y. Go ^{29,h}

- M. Goblirsch-Kolb³⁶, B. Gocke⁴⁹, D. Godin¹⁰⁸, B. Gokturk^{21a}, S. Goldfarb¹⁰⁵, T. Golling⁵⁶, M. G. D. Gololo^{33g}, D. Golubkov³⁷, J. P. Gombas¹⁰⁷, A. Gomes^{130a,130b}, G. Gomes Da Silva¹⁴¹, A. J. Gomez Delegido¹⁶³, R. Gonçalo^{130a,130c}, G. Gonella¹²³, L. Gonella²⁰, A. Gongadze³⁸, F. Gonnella²⁰, J. L. Gonski⁴¹, R. Y. González Andana⁵², S. González de la Hoz¹⁶³, S. Gonzalez Fernandez¹³, R. Gonzalez Lopez⁹², C. Gonzalez Renteria^{17a}, R. Gonzalez Suarez¹⁶¹, S. Gonzalez-Sevilla⁵⁶, G. R. Gonzalvo Rodriguez¹⁶³, L. Goossens³⁶, P. A. Gorbounov³⁷, B. Gorini³⁶, E. Gorini^{70a,70b}, A. Gorišek⁹³, T. C. Gosart¹²⁸, A. T. Goshaw⁵¹, M. I. Gostkin³⁸, S. Goswami¹²¹, C. A. Gottardo³⁶, M. Gouighri^{35b}, V. Goumarre⁴⁸, A. G. Goussiou¹³⁸, N. Govender^{33c}, I. Grabowska-Bold^{85a}, K. Graham³⁴, E. Gramstad¹²⁵, S. Grancagnolo^{70a,70b}, M. Grandi¹⁴⁶, V. Gratchev^{37,i}, P. M. Gravila^{27f}, F. G. Gravili^{70a,70b}, H. M. Gray^{17a}, M. Greco^{70a,70b}, C. Greife²⁴, I. M. Gregor⁴⁸, P. Grenier¹⁴³, C. Grieco¹³, A. A. Grillo¹³⁶, K. Grimm^{31,w}, S. Grinstein^{13,x}, J.-F. Grivaz⁶⁶, E. Gross¹⁶⁹, J. Grosse-Knetter⁵⁵, C. Grud¹⁰⁶, J. C. Grundy¹²⁶, L. Guan¹⁰⁶, W. Guan¹⁷⁰, C. Gubbels¹⁶⁴, J. G.R. Guerrero Rojas¹⁶³, G. Guerrieri^{69a,69b}, F. Guescini¹¹⁰, R. Gugel¹⁰⁰, J. A. M. Guhit¹⁰⁶, A. Guida⁴⁸, T. Guillemain⁴, E. Guillon^{167,134}, S. Guindon³⁶, F. Guo^{14a,14e}, J. Guo^{62c}, L. Guo⁶⁶, Y. Guo¹⁰⁶, R. Gupta⁴⁸, S. Gurbuz²⁴, S. S. Gurdasani⁵⁴, G. Gustavino³⁶, M. Guth⁵⁶, P. Gutierrez¹²⁰, L. F. Gutierrez Zagazeta¹²⁸, C. Gutscheow⁹⁶, C. Gwenlan¹²⁶, C. B. Gwilliam⁹², E. S. Haaland¹²⁵, A. Haas¹¹⁷, M. Habedank⁴⁸, C. Haber^{17a}, H. K. Hadavand⁸, A. Hadeef¹⁰⁰, S. Hadzic¹¹⁰, J. J. Hahn¹⁴¹, E. H. Haines⁹⁶, M. Haleem¹⁶⁶, J. Haley¹²¹, J. J. Hall¹³⁹, G. D. Hallewell¹⁰², L. Halser¹⁹, K. Hamano¹⁶⁵, H. Hamdaoui^{35e}, M. Hamer²⁴, G. N. Hamity⁵², E. J. Hampshire⁹⁵, J. Han^{62b}, K. Han^{62a}, L. Han^{14c}, L. Han^{62a}, S. Han^{17a}, Y. F. Han¹⁵⁵, K. Hanagaki⁸³, M. Hance¹³⁶, D. A. Hangal^{41,c}, H. Hanif¹⁴², M. D. Hank¹²⁸, R. Hankache¹⁰¹, J. B. Hansen⁴², J. D. Hansen⁴², P. H. Hansen⁴², K. Hara¹⁵⁷, D. Harada⁵⁶, T. Harenberg¹⁷¹, S. Harkusha³⁷, Y. T. Harris¹²⁶, N. M. Harrison¹¹⁹, P. F. Harrison¹⁶⁷, N. M. Hartman¹⁴³, N. M. Hartmann¹⁰⁹, Y. Hasegawa¹⁴⁰, A. Hasib⁵², S. Haug¹⁹, R. Hauser¹⁰⁷, M. Havranek¹³², C. M. Hawkes²⁰, R. J. Hawkings³⁶, Y. Hayashi¹⁵³, S. Hayashida¹¹¹, D. Hayden¹⁰⁷, C. Hayes¹⁰⁶, R. L. Hayes¹¹⁴, C. P. Hays¹²⁶, J. M. Hays⁹⁴, H. S. Hayward⁹², F. He^{62a}, Y. He¹⁵⁴, Y. He¹²⁷, N. B. Heatley⁹⁴, V. Hedberg⁹⁸, A. L. Heggelund¹²⁵, N. D. Hehir⁹⁴, C. Heidegger⁵⁴, K. K. Heidegger⁵⁴, W. D. Heidorn⁸¹, J. Heilman³⁴, S. Heim⁴⁸, T. Heim^{17a}, C. G. Heinlein¹²⁸, J. J. Heinrich¹²³, L. Heinrich^{110,y}, J. Hejbal¹³¹, L. Helary⁴⁸, A. Held¹⁷⁰, S. Hellesund¹⁶, C. M. Helling¹⁶⁴, S. Hellman^{47a,47b}, C. Helsen³⁶, R. C. W. Henderson⁹¹, L. Henkelmann³², A. M. Henriques Correia³⁶, H. Herde⁹⁸, Y. Hernández Jiménez¹⁴⁵, L. M. Herrmann²⁴, T. Herrmann⁵⁰, G. Herten⁵⁴, R. Hertenberger¹⁰⁹, L. Hervas³⁶, N. P. Hessey^{156a}, H. Hibi⁸⁴, S. J. Hillier²⁰, F. Hinterkeuser²⁴, M. Hirose¹²⁴, S. Hirose¹⁵⁷, D. Hirschbuehl¹⁷¹, T. G. Hitchings¹⁰¹, B. Hiti⁹³, J. Hobbs¹⁴⁵, R. Hobincu^{27e}, N. Hod¹⁶⁹, M. C. Hodgkinson¹³⁹, B. H. Hodgkinson³², A. Hoecker³⁶, J. Hofer⁴⁸, T. Holm²⁴, M. Holzbock¹¹⁰, L. B.A.H. Hommels³², B. P. Honan¹⁰¹, J. Hong^{62c}, T. M. Hong¹²⁹, J. C. Honig⁵⁴, B. H. Hooberman¹⁶², W. H. Hopkins⁶, Y. Horii¹¹¹, S. Hou¹⁴⁸, A. S. Howard⁹³, J. Howarth⁵⁹, J. Hoya⁶, M. Hrabovsky¹²², A. Hrynevich⁴⁸, T. Hryn'ova⁴, P. J. Hsu⁶⁵, S.-C. Hsu¹³⁸, Q. Hu⁴¹, Y. F. Hu^{14a,14e}, D. P. Huang⁹⁶, S. Huang^{64b}, X. Huang^{14c}, Y. Huang^{62a}, Y. Huang^{14a}, Z. Huang¹⁰¹, Z. Hubacek¹³², M. Huebner²⁴, F. Huegging²⁴, T. B. Huffman¹²⁶, C. A. Hugli⁴⁸, M. Huhtinen³⁶, S. K. Huiberts¹⁶, R. Hulsken¹⁰⁴, N. Huseynov^{12,i}, J. Huston¹⁰⁷, J. Huth⁶¹, R. Hyneman¹⁴³, G. Iacobucci⁵⁶, G. Iakovidis²⁹, I. Ibragimov¹⁴¹, L. Iconomidou-Fayard⁶⁶, P. Iengo^{72a,72b}, R. Iguchi¹⁵³, T. Iizawa⁵⁶, Y. Ikegami⁸³, A. Ilg¹⁹, N. Ilic¹⁵⁵, H. Imam^{35a}, T. Ingebretsen Carlson^{47a,47b}, G. Introzzi^{73a,73b}, M. Iodice^{77a}, V. Ippolito^{75a,75b}, M. Ishino¹⁵³, W. Islam¹⁷⁰, C. Issever^{18,48}, S. Istin^{21a,z}, H. Ito¹⁶⁸, J. M. Iturbe Ponce^{64a}, R. Iuppa^{78a,78b}, A. Ivina¹⁶⁹, J. M. Izen⁴⁵, V. Izzo^{72a}, P. Jacka^{131,132}, P. Jackson¹, R. M. Jacobs⁴⁸, B. P. Jaeger¹⁴², C. S. Jagfeld¹⁰⁹, P. Jain⁵⁴, G. Jäkel¹⁷¹, K. Jakobs⁵⁴, T. Jakoubek¹⁶⁹, J. Jamieson⁵⁹, K. W. Janas^{85a}, A. E. Jaspan⁹², M. Javurkova¹⁰³, F. Jeanneau¹³⁵, L. Jeanty¹²³, J. Jeljela^{149a,aa}, P. Jenni^{54,ab}, C. E. Jessiman³⁴, S. Jézéquel⁴, C. Jia^{62b}, J. Jia¹⁴⁵, X. Jia⁶¹, X. Jia^{14a,14e}, Z. Jia^{14c}, Y. Jiang^{62a}, S. Jiggins⁴⁸, J. Jimenez Pena¹¹⁰, S. Jin^{14c}, A. Jinaru^{27b}, O. Jinnouchi¹⁵⁴, P. Johansson¹³⁹, K. A. Johns⁷, J. W. Johnson¹³⁶, D. M. Jones³², E. Jones⁴⁸, P. Jones³², R. W. L. Jones⁹¹, T. J. Jones⁹², R. Joshi¹¹⁹, J. Jovicevic¹⁵, X. Ju^{17a}, J. J. Junggeburth³⁶, T. Junkermann^{63a}, A. Juste Rozas^{13,x}, S. Kabana^{137e}, A. Kaczmarska⁸⁶, M. Kado¹¹⁰, H. Kagan¹¹⁹, M. Kagan¹⁴³, A. Kahn⁴¹, A. Kahn¹²⁸, C. Kahra¹⁰⁰, T. Kaji¹⁶⁸, E. Kajomovitz¹⁵⁰, N. Kakati¹⁶⁹, C. W. Kalderon²⁹, A. Kamenshchikov¹⁵⁵, S. Kanayama¹⁵⁴, N. J. Kang¹³⁶, D. Kar^{33g}, K. Karava¹²⁶, M. J. Kareem^{156b}, E. Karentzos⁵⁴, I. Karkanas^{152,ac}, S. N. Karpov³⁸, Z. M. Karpova³⁸, V. Kartvelishvili⁹¹, A. N. Karyukhin³⁷, E. Kasimi^{152,ac}, J. Katzy⁴⁸, S. Kaur³⁴, K. Kawade¹⁴⁰, T. Kawamoto¹³⁵, E. F. Kay³⁶, F. I. Kaya¹⁵⁸, S. Kazakos¹³, V. F. Kazanin³⁷, Y. Ke¹⁴⁵, J. M. Keaveney^{33a}, R. Keeler¹⁶⁵, G. V. Kehris⁶¹, J. S. Keller³⁴, A. S. Kelly⁹⁶, D. Kelsey¹⁴⁶, J. J. Kempster¹⁴⁶, K. E. Kennedy⁴¹, P. D. Kennedy¹⁰⁰, O. Kepka¹³¹, B. P. Kerridge¹⁶⁷, S. Kersten¹⁷¹, B. P. Kerševan⁹³, S. Keshri⁶⁶, L. Keszezhova^{28a}, S. Ketabchi Haghighat¹⁵⁵, M. Khandoga¹²⁷, A. Khanov¹²¹, A. G. Kharlamov³⁷, T. Kharlamova³⁷, E. E. Khoda¹³⁸, T. J. Khoo¹⁸, G. Khoriuli¹⁶⁶, J. Khubua^{149b}, Y. A. R. Khwaira⁶⁶, M. Kiehn³⁶, A. Kilgallon¹²³, D. W. Kim^{47a,47b}, Y. K. Kim³⁹, N. Kimura⁹⁶, A. Kirchoff⁵⁵, C. Kirfel²⁴, J. Kirk¹³⁴, A. E. Kiryunin¹¹⁰, D. P. Kisiuk¹⁵⁵, C. Kitsaki¹⁰, O. Kivernyk²⁴, M. Klassen^{63a}, C. Klein³⁴, L. Klein¹⁶⁶, M. H. Klein¹⁰⁶, M. Klein⁹², S. B. Klein⁵⁶, U. Klein⁹², P. Klimek³⁶, A. Klimentov²⁹, T. Klioutchnikova³⁶, P. Kluit¹¹⁴, S. Kluth¹¹⁰, E. Kneringer⁷⁹, T. M. Knight¹⁵⁵, A. Knue⁵⁴, R. Kobayashi⁸⁷, S. F. Koch¹²⁶

M. Kocian¹⁴³, P. Kodyš¹³³, D. M. Koeck¹²³, P. T. Koenig²⁴, T. Koffas³⁴, M. Kolb¹³⁵, I. Koletsou⁴, T. Komarek¹²², K. Köneke⁵⁴, A. X. Y. Kong¹, T. Kono¹¹⁸, N. Konstantinidis⁹⁶, B. Konya⁹⁸, R. Kopeliansky⁶⁸, S. Koperny^{85a}, K. Korcyl⁸⁶, K. Kordas^{152,ac}, G. Koren¹⁵¹, A. Korn⁹⁶, S. Korn⁵⁵, I. Korolkov¹³, N. Korotkova³⁷, B. Kortman¹¹⁴, O. Kortner¹¹⁰, S. Kortner¹¹⁰, W. H. Kostecka¹¹⁵, V. V. Kostyukhin¹⁴¹, A. Kotskechagia¹³⁵, A. Kotwal⁵¹, A. Koulouris³⁶, A. Kourkoumeli-Charalampidi^{73a,73b}, C. Kourkoumelis⁹, E. Kourlitis⁶, O. Kovanda¹⁴⁶, R. Kowalewski¹⁶⁵, W. Kozanecki¹³⁵, A. S. Kozhin³⁷, V. A. Kramarenko³⁷, G. Kramberger⁹³, P. Kramer¹⁰⁰, M. W. Krasny¹²⁷, A. Krasznahorkay³⁶, J. A. Kremer¹⁰⁰, T. Kresse⁵⁰, J. Kretzschmar⁹², K. Kreul¹⁸, P. Krieger¹⁵⁵, S. Krishnamurthy¹⁰³, M. Krivos¹³³, K. Krizka²⁰, K. Kroeninger⁴⁹, H. Kroha¹¹⁰, J. Kroll¹³¹, J. Kroll¹²⁸, K. S. Krowpman¹⁰⁷, U. Kruchonak³⁸, H. Krüger²⁴, N. Krumnack⁸¹, M. C. Kruse⁵¹, J. A. Krzysiak⁸⁶, O. Kuchinskaja³⁷, S. Kудay^{3a}, S. Kuehn³⁶, R. Kuesters⁵⁴, T. Kuhl⁴⁸, V. Kukhtin³⁸, Y. Kulchitsky^{37,1}, S. Kuleshov^{137d,137b}, M. Kumar^{33g}, N. Kumari¹⁰², A. Kupco¹³¹, T. Kupfer⁴⁹, A. Kupich³⁷, O. Kuprash⁵⁴, H. Kurashige⁸⁴, L. L. Kurchaninov^{156a}, O. Kurdysh⁶⁶, Y. A. Kurochkin³⁷, A. Kurova³⁷, M. Kuze¹⁵⁴, A. K. Kvam¹⁰³, J. Kvita¹²², T. Kwan¹⁰⁴, N. G. Kyriacou¹⁰⁶, L. A. O. Laatu¹⁰², C. Lacasta¹⁶³, F. Lacava^{75a,75b}, H. Lacker¹⁸, D. Lacour¹²⁷, N. N. Lad⁹⁶, E. Ladygin³⁸, B. Laforge¹²⁷, T. Lagouri^{137e}, S. Lai⁵⁵, I. K. Lakomic^{85a}, N. Lalloue⁶⁰, J. E. Lambert¹²⁰, S. Lammers⁶⁸, W. Lampl⁷, C. Lampoudis^{152,ac}, A. N. Lancaster¹¹⁵, E. Lançon²⁹, U. Landgraf⁵⁴, M. P. J. Landon⁹⁴, V. S. Lang⁵⁴, R. J. Langenberg¹⁰³, O. K. B. Langrekken¹²⁵, A. J. Lankford¹⁶⁰, F. Lanni³⁶, K. Lantsch²⁴, A. Lanza^{73a}, A. Lapertosa^{57b,57a}, J. F. Laporte¹³⁵, T. Lari^{71a}, F. Lasagni Manghi^{23b}, M. Lassnig³⁶, V. Latonova¹³¹, A. Laudrain¹⁰⁰, A. Laurier¹⁵⁰, S. D. Lawlor⁹⁵, Z. Lawrence¹⁰¹, M. Lazzaroni^{71a,71b}, B. Le¹⁰¹, E. M. Le Boulicaut⁵¹, B. Leban⁹³, A. Lebedev⁸¹, M. LeBlanc³⁶, F. Ledroit-Guillon⁶⁰, A. C. A. Lee⁹⁶, G. R. Lee¹⁶, S. C. Lee¹⁴⁸, S. Lee^{47a,47b}, T. F. Lee⁹², L. L. Leeuw^{33c}, H. P. Lefebvre⁹⁵, M. Lefebvre¹⁶⁵, C. Leggett^{17a}, K. Lehmann¹⁴², G. Lehmann Miotto³⁶, M. Leigh⁵⁶, W. A. Light¹⁰³, A. Leisos^{152,ad}, M. A. L. Leite^{82c}, C. E. Leitgeb⁴⁸, R. Leitner¹³³, K. J. C. Leney⁴⁴, T. Lenz²⁴, S. Leone^{74a}, C. Leonidopoulos⁵², A. Leopold¹⁴⁴, C. Leroy¹⁰⁸, R. Les¹⁰⁷, C. G. Lester³², M. Levchenko³⁷, J. Levêque⁴, D. Levin¹⁰⁶, L. J. Levinson¹⁶⁹, M. P. Lewicki⁸⁶, D. J. Lewis⁴, A. Li⁵, B. Li^{62b}, C. Li^{62a}, C-Q. Li^{62c}, H. Li^{62a}, H. Li^{62b}, H. Li^{14c}, H. Li^{62b}, J. Li^{62c}, L. Li^{62c}, M. Li^{14a,14e}, Q. Y. Li^{62a}, S. Li^{14a,14e}, S. Li^{62d,62c,ae}, T. Li^{62b}, X. Li¹⁰⁴, Z. Li^{62b}, Z. Li¹²⁶, Z. Li¹⁰⁴, Z. Li⁹², Z. Li^{14a,14e}, Z. Liang^{14a}, M. Liberatore⁴⁸, B. Liberti^{76a}, K. Lie^{64c}, J. Lieber Marin^{82b}, H. Lien⁶⁸, K. Lin¹⁰⁷, R. A. Linck⁶⁸, R. E. Lindley⁷, J. H. Lindon², A. Linss⁴⁸, E. Lipeles¹²⁸, A. Lipniacka¹⁶, A. Lister¹⁶⁴, J. D. Little⁴, B. Liu^{14a}, B. X. Liu¹⁴², D. Liu^{62d,62c}, J. B. Liu^{62a}, J. K. K. Liu³², K. Liu^{62d,62c}, M. Liu^{62a}, M. Y. Liu^{62a}, P. Liu^{14a}, Q. Liu^{62d,138,62c}, X. Liu^{62a}, Y. Liu^{14d,14e}, Y. L. Liu¹⁰⁶, Y. W. Liu^{62a}, J. Llorente Merino¹⁴², S. L. Lloyd⁹⁴, E. M. Lobodzinska⁴⁸, P. Loch⁷, S. Loffredo^{76a,76b}, T. Lohse¹⁸, K. Lohwasser¹³⁹, E. Loiacono⁴⁸, M. Lokajicek^{131,i}, J. D. Lomas²⁰, J. D. Long¹⁶², I. Longarini¹⁶⁰, L. Longo^{70a,70b}, R. Longo¹⁶², I. Lopez Paz⁶⁷, A. Lopez Solis⁴⁸, J. Lorenz¹⁰⁹, N. Lorenzo Martinez⁴, A. M. Lory¹⁰⁹, X. Lou^{47a,47b}, X. Lou^{14a,14e}, A. Lounis⁶⁶, J. Love⁶, P. A. Love⁹¹, G. Lu^{14a,14e}, M. Lu⁸⁰, S. Lu¹²⁸, Y. J. Lu⁶⁵, H. J. Lubatti¹³⁸, C. Luci^{75a,75b}, F. L. Lucio Alves^{14c}, A. Lucotte⁶⁰, F. Luehring⁶⁸, I. Luise¹⁴⁵, O. Lukianchuk⁶⁶, O. Lundberg¹⁴⁴, B. Lund-Jensen¹⁴⁴, N. A. Luongo¹²³, M. S. Lutz¹⁵¹, D. Lynn²⁹, H. Lyons⁹², R. Lysak¹³¹, E. Lytken⁹⁸, V. Lyubushkin³⁸, T. Lyubushkina³⁸, M. M. Lyukova¹⁴⁵, H. Ma²⁹, L. L. Ma^{62b}, Y. Ma⁹⁶, D. M. Mac Donell¹⁶⁵, G. Maccarrone⁵³, J. C. MacDonald¹³⁹, R. Madar⁴⁰, W. F. Mader⁵⁰, J. Maeda⁸⁴, T. Maeno²⁹, M. Maerker⁵⁰, H. Maguire¹³⁹, A. Maio^{130a,130b,130d}, K. Maj^{85a}, O. Majersky⁴⁸, S. Majewski¹²³, N. Makovec⁶⁶, V. Maksimovic¹⁵, B. Malaescu¹²⁷, Pa. Malecki⁸⁶, V. P. Maleev³⁷, F. Malek⁶⁰, D. Malito^{43b,43a}, U. Mallik⁸⁰, C. Malone³², S. Maltezos¹⁰, S. Malyukov³⁸, J. Mamuzic¹³, G. Mancini⁵³, G. Manco^{73a,73b}, J. P. Mandalia⁹⁴, I. Mandić⁹³, L. Manhaes de Andrade Filho^{82a}, I. M. Maniatis¹⁶⁹, J. Manjarres Ramos^{102,af}, D. C. Mankad¹⁶⁹, A. Mann¹⁰⁹, B. Mansoulie¹³⁵, S. Manzoni³⁶, A. Marantis^{152,ad}, G. Marchiori⁵, M. Marcisovsky¹³¹, C. Marcon^{71a,71b}, M. Marinescu²⁰, M. Marjanovic¹²⁰, E. J. Marshall⁹¹, Z. Marshall^{17a}, S. Marti-Garcia¹⁶³, T. A. Martin¹⁶⁷, V. J. Martin⁵², B. Martin dit Latour¹⁶, L. Martinelli^{75a,75b}, M. Martinez^{13,x}, P. Martinez Agullo¹⁶³, V. I. Martinez Outschoorn¹⁰³, P. Martinez Suarez¹³, S. Martin-Haugh¹³⁴, V. S. Martoiu^{27b}, A. C. Martyniuk⁹⁶, A. Marzin³⁶, S. R. Maschek¹¹⁰, D. Mascione^{78a,78b}, L. Masetti¹⁰⁰, T. Mashimo¹⁵³, J. Masik¹⁰¹, A. L. Maslennikov³⁷, L. Massa^{23b}, P. Massarotti^{72a,72b}, P. Mastrandrea^{74a,74b}, A. Mastroberardino^{43b,43a}, T. Masubuchi¹⁵³, T. Mathisen¹⁶¹, J. Matousek¹³³, N. Matsuzawa¹⁵³, J. Maurer^{27b}, B. Maček⁹³, D. A. Maximov³⁷, R. Mazini¹⁴⁸, I. Maznas^{152,ac}, M. Mazza¹⁰⁷, S. M. Mazza¹³⁶, C. Mc Ginn²⁹, J. P. Mc Gowan¹⁰⁴, S. P. Mc Kee¹⁰⁶, E. F. McDonald¹⁰⁵, A. E. McDougall¹¹⁴, J. A. Mcfayden¹⁴⁶, R. P. McGovern¹²⁸, G. Mchedlidze^{149b}, R. P. McKenzie^{33g}, T. C. Mclachlan⁴⁸, D. J. McLaughlin⁹⁶, K. D. McLean¹⁶⁵, S. J. McMahon¹³⁴, P. C. McNamara¹⁰⁵, C. M. Mcpartland⁹², R. A. McPherson^{165,p}, T. Megy⁴⁰, S. Mehlhase¹⁰⁹, A. Mehta⁹², D. Melini¹⁵⁰, B. R. Mellado Garcia^{33g}, A. H. Melo⁵⁵, F. Meloni⁴⁸, A. M. Mendes Jacques Da Costa¹⁰¹, H. Y. Meng¹⁵⁵, L. Meng⁹¹, S. Menke¹¹⁰, M. Mentink³⁶, E. Meoni^{43b,43a}, C. Merlassino¹²⁶, L. Merola^{72a,72b}, C. Meroni^{71a}, G. Merz¹⁰⁶, O. Meshkov³⁷, J. Metcalfe⁶, A. S. Mete⁶, C. Meyer⁶⁸, J-P. Meyer¹³⁵, R. P. Middleton¹³⁴, L. Mijović⁵², G. Mikenberg¹⁶⁹, M. Mikesstikova¹³¹, M. Mikuž⁹³, H. Mildner¹³⁹, A. Milic³⁶, C. D. Milke⁴⁴, D. W. Miller³⁹, L. S. Miller³⁴, A. Milov¹⁶⁹, D. A. Milstead^{47a,47b}, T. Min^{14c}, A. A. Minaenko³⁷

- I. A. Minashvili ^{149b}, L. Mince ⁵⁹, A. I. Mincer ¹¹⁷, B. Mindur ^{85a}, M. Mineev ³⁸, Y. Mino ⁸⁷, L. M. Mir ¹³, M. Miralles Lopez ¹⁶³, M. Mironova ^{17a}, A. Mishima ¹⁵³, M. C. Missio ¹¹³, T. Mitani ¹⁶⁸, A. Mitra ¹⁶⁷, V. A. Mitsou ¹⁶³, O. Miu ¹⁵⁵, P. S. Miyagawa ⁹⁴, Y. Miyazaki ⁸⁹, A. Mizukami ⁸³, T. Mkrtychyan ^{63a}, M. Mlinarevic ⁹⁶, T. Mlinarevic ⁹⁶, M. Mlynarikova ³⁶, S. Mobius ⁵⁵, K. Mochizuki ¹⁰⁸, P. Moder ⁴⁸, P. Mogg ¹⁰⁹, A. F. Mohammed ^{14a,14e}, S. Mohapatra ⁴¹, G. Mokgatitswane ^{33g}, B. Mondal ¹⁴¹, S. Mondal ¹³², G. Monig ¹⁴⁶, K. Mönig ⁴⁸, E. Monnier ¹⁰², L. Monsonis Romero ¹⁶³, J. Montejo Berlingen ⁸³, M. Montella ¹¹⁹, F. Monticelli ⁹⁰, N. Morange ⁶⁶, A. L. Moreira De Carvalho ^{130a}, M. Moreno Llácer ¹⁶³, C. Moreno Martinez ⁵⁶, P. Morettini ^{57b}, S. Morgenstern ³⁶, M. Morii ⁶¹, M. Morinaga ¹⁵³, A. K. Morley ³⁶, F. Morodei ^{75a,75b}, L. Morvaj ³⁶, P. Moschovakos ³⁶, B. Moser ³⁶, M. Mosidze ^{149b}, T. Moskalets ⁵⁴, P. Moskvitina ¹¹³, J. Moss ^{31,ag}, E. J. W. Moyses ¹⁰³, O. Mtintsilana ^{33g}, S. Muanza ¹⁰², J. Mueller ¹²⁹, D. Muenstermann ⁹¹, R. Müller ¹⁹, G. A. Mullier ¹⁶¹, J. J. Mullin ¹²⁸, D. P. Mungo ¹⁵⁵, D. Munoz Perez ¹⁶³, F. J. Munoz Sanchez ¹⁰¹, M. Murin ¹⁰¹, W. J. Murray ^{167,134}, A. Murrone ^{71a,71b}, J. M. Muse ¹²⁰, M. Muškinja ^{17a}, C. Mwewa ²⁹, A. G. Myagkov ^{37,1}, A. J. Myers ⁸, A. A. Myers ¹²⁹, G. Myers ⁶⁸, M. Myska ¹³², B. P. Nachman ^{17a}, O. Nackenhorst ⁴⁹, A. Nag ⁵⁰, K. Nagai ¹²⁶, K. Nagano ⁸³, J. L. Nagle ^{29,h}, E. Nagy ¹⁰², A. M. Nairz ³⁶, Y. Nakahama ⁸³, K. Nakamura ⁸³, H. Nanjo ¹²⁴, R. Narayan ⁴⁴, E. A. Narayanan ¹¹², I. Naryshkin ³⁷, M. Naseri ³⁴, S. Nasri ¹⁵⁹, C. Nass ²⁴, G. Navarro ^{22a}, J. Navarro-Gonzalez ¹⁶³, R. Nayak ¹⁵¹, A. Nayaz ¹⁸, P. Y. Nechaeva ³⁷, F. Nechansky ⁴⁸, L. Nedic ¹²⁶, T. J. Neep ²⁰, A. Negri ^{73a,73b}, M. Negrini ^{23b}, C. Nellist ¹¹⁴, C. Nelson ¹⁰⁴, K. Nelson ¹⁰⁶, S. Nemecek ¹³¹, M. Nessi ^{36,ah}, M. S. Neubauer ¹⁶², F. Neuhaus ¹⁰⁰, J. Neundorff ⁴⁸, R. Newhouse ¹⁶⁴, P. R. Newman ²⁰, C. W. Ng ¹²⁹, Y. W. Y. Ng ⁴⁸, B. Ngair ^{35e}, H. D. N. Nguyen ¹⁰⁸, R. B. Nickerson ¹²⁶, R. Nicolaidou ¹³⁵, J. Nielsen ¹³⁶, M. Niemeyer ⁵⁵, J. Niemann ^{55,36}, N. Nikiforou ³⁶, V. Nikolaenko ^{37,1}, I. Nikolic-Audit ¹²⁷, K. Nikolopoulos ²⁰, P. Nilsson ²⁹, I. Ninca ⁴⁸, H. R. Nindhito ⁵⁶, G. Ninio ¹⁵¹, A. Nisati ^{75a}, N. Nishu ², R. Nisius ¹¹⁰, J.-E. Nitschke ⁵⁰, E. K. Nkadimeng ^{33g}, S. J. Noacco Rosende ⁹⁰, T. Nobe ¹⁵³, D. L. Noel ³², T. Nommensen ¹⁴⁷, M. A. Nomura ²⁹, M. B. Norfolk ¹³⁹, R. R. B. Norisam ⁹⁶, B. J. Norman ³⁴, J. Novak ⁹³, T. Novak ⁴⁸, L. Novotny ¹³², R. Novotny ¹¹², L. Nozka ¹²², K. Ntekas ¹⁶⁰, N. M.J. Nunes De Moura Junior ^{82b}, E. Nurse ⁹⁶, J. Ocariz ¹²⁷, A. Ochi ⁸⁴, I. Ochoa ^{130a}, S. Oerdek ¹⁶¹, J. T. Offermann ³⁹, A. Ogrodnik ^{85a}, A. Oh ¹⁰¹, C. C. Ohm ¹⁴⁴, H. Oide ⁸³, R. Oishi ¹⁵³, M. L. Ojeda ⁴⁸, Y. Okazaki ⁸⁷, M. W. O'Keefe ⁹², Y. Okumura ¹⁵³, L. F. Oleiro Seabra ^{130a}, S. A. Olivares Pino ^{137d}, D. Oliveira Damazio ²⁹, D. Oliveira Goncalves ^{82a}, J. L. Oliver ¹⁶⁰, M. J. R. Olsson ¹⁶⁰, A. Olszewski ⁸⁶, Ö.O. Öncel ⁵⁴, D. C. O'Neil ¹⁴², A. P. O'Neill ¹⁹, A. Onofre ^{130a,130e}, P. U. E. Onyisi ¹¹, M. J. Oreglia ³⁹, G. E. Orellana ⁹⁰, D. Orestano ^{77a,77b}, N. Orlando ¹³, R. S. Orr ¹⁵⁵, V. O'Shea ⁵⁹, R. Ospanov ^{62a}, G. Otero y Garzon ³⁰, H. Otono ⁸⁹, P. S. Ott ^{63a}, G. J. Ottino ^{17a}, M. Ouchrif ^{35d}, J. Ouellette ²⁹, F. Ould-Saada ¹²⁵, M. Owen ⁵⁹, R. E. Owen ¹³⁴, K. Y. Oyulmaz ^{21a}, V. E. Ozcan ^{21a}, N. Ozturk ⁸, S. Ozturk ^{21d}, H. A. Pacey ³², A. Pacheco Pages ¹³, C. Padilla Aranda ¹³, G. Padovano ^{75a,75b}, S. Pagan Griso ^{17a}, G. Palacino ⁶⁸, A. Palazzo ^{70a,70b}, S. Palestini ³⁶, J. Pan ¹⁷², T. Pan ^{64a}, D. K. Panchal ¹¹, C. E. Pandini ¹¹⁴, J. G. Panduro Vazquez ⁹⁵, H. Pang ^{14b}, P. Pani ⁴⁸, G. Panizzo ^{69a,69c}, L. Paolozzi ⁵⁶, C. Papadatos ¹⁰⁸, S. Parajuli ⁴⁴, A. Paramonov ⁶, C. Paraskevopoulos ¹⁰, D. Paredes Hernandez ^{64b}, T. H. Park ¹⁵⁵, M. A. Parker ³², F. Parodi ^{57b,57a}, E. W. Parrish ¹¹⁵, V. A. Parrish ⁵², J. A. Parsons ⁴¹, U. Parzefall ⁵⁴, B. Pascual Dias ¹⁰⁸, L. Pascual Dominguez ¹⁵¹, F. Pasquali ¹¹⁴, E. Pasqualucci ^{75a}, S. Passaggio ^{57b}, F. Pastore ⁹⁵, P. Pasuwan ^{47a,47b}, P. Patel ⁸⁶, U. M. Patel ⁵¹, J. R. Pater ¹⁰¹, T. Pauly ³⁶, J. Parkes ¹⁴³, M. Pedersen ¹²⁵, R. Pedro ^{130a}, S. V. Peleganchuk ³⁷, O. Penc ³⁶, E. A. Pender ⁵², H. Peng ^{62a}, K. E. Pinski ¹⁰⁹, M. Penzin ³⁷, B. S. Peralva ^{82d}, A. P. Pereira Peixoto ⁶⁰, L. Pereira Sanchez ^{47a,47b}, D. V. Perpelitsa ^{29,h}, E. Perez Codina ^{156a}, M. Perganti ¹⁰, L. Perini ^{71a,71b,i}, H. Pernegger ³⁶, S. Perrella ³⁶, A. Perrevoort ¹¹³, O. Perrin ⁴⁰, K. Peters ⁴⁸, R. F. Y. Peters ¹⁰¹, B. A. Petersen ³⁶, T. C. Petersen ⁴², E. Petit ¹⁰², V. Petousis ¹³², C. Petridou ^{152,ac}, A. Petrukhin ¹⁴¹, M. Pettee ^{17a}, N. E. Pettersson ³⁶, A. Petukhov ³⁷, K. Petukhova ¹³³, A. Peyaud ¹³⁵, R. Pezoa ^{137f}, L. Pezzotti ³⁶, G. Pezzullo ¹⁷², T. M. Pham ¹⁷⁰, T. Pham ¹⁰⁵, P. W. Phillips ¹³⁴, M. W. Phipps ¹⁶², G. Piacquadio ¹⁴⁵, E. Pianori ^{17a}, F. Piazza ^{71a,71b}, R. Piegai ³⁰, D. Pietreanu ^{27b}, A. D. Pilkington ¹⁰¹, M. Pinamonti ^{69a,69c}, J. L. Pinfold ², B. C. Pinheiro Pereira ^{130a}, A. E. Pinto Pinoargote ¹³⁵, C. Pitman Donaldson ⁹⁶, D. A. Pizzi ³⁴, L. Pizzimento ^{76a,76b}, A. Pizzini ¹¹⁴, M.-A. Pleier ²⁹, V. Plesanovs ⁵⁴, V. Pleskot ¹³³, E. Plotnikova ³⁸, G. Poddar ⁴, R. Poettgen ⁹⁸, L. Poggioli ¹²⁷, D. Pohl ²⁴, I. Pokharel ⁵⁵, S. Polacek ¹³³, G. Polesello ^{73a}, A. Poley ^{142,156a}, R. Polifka ¹³², A. Polini ^{23b}, C. S. Pollard ¹⁶⁷, Z. B. Pollock ¹¹⁹, V. Polychronakos ²⁹, E. Pompa Pacchi ^{75a,75b}, D. Ponomarenko ¹¹³, L. Pontecorvo ³⁶, S. Popa ^{27a}, G. A. Popeneciu ^{27d}, D. M. Portillo Quintero ^{156a}, S. Pospisil ¹³², P. Postolache ^{27c}, K. Potamianos ¹²⁶, P. P. Potepa ^{85a}, I. N. Potrap ³⁸, C. J. Potter ³², H. Potti ¹, T. Poulsen ⁴⁸, J. Poveda ¹⁶³, M. E. Pozo Astigarraga ³⁶, A. Prades Ibanez ¹⁶³, M. M. Prapa ⁴⁶, J. Pretel ⁵⁴, D. Price ¹⁰¹, M. Primavera ^{70a}, M. A. Principe Martin ⁹⁹, R. Privara ¹²², T. Procter ⁵⁹, M. L. Proffitt ¹³⁸, N. Proklova ¹²⁸, K. Prokofiev ^{64c}, G. Proto ^{76a,76b}, S. Protopopescu ²⁹, J. Proudfoot ⁶, M. Przybycien ^{85a}, W. W. Przygoda ^{85b}, J. E. Puddefoot ¹³⁹, D. Pudzha ³⁷, D. Pyatiizbyantseva ³⁷, J. Qian ¹⁰⁶, D. Qichen ¹⁰¹, Y. Qin ¹⁰¹, T. Qiu ⁵², A. Quadt ⁵⁵, M. Queitsch-Maitland ¹⁰¹, G. Quetant ⁵⁶, G. Rabanal Bolanos ⁶¹, D. Rafanoharana ⁵⁴, F. Ragusa ^{71a,71b}, J. L. Rainbolt ³⁹, J. A. Raine ⁵⁶, S. Rajagopalan ²⁹, E. Ramakoti ³⁷, K. Ran ^{48,14e}, N. P. Rapheeha ^{33g}, H. Rasheed ^{27b}, V. Raskina ¹²⁷, D. F. Rassloff ^{63a}, S. Rave ¹⁰⁰, B. Ravina ⁵⁵, I. Ravinovich ¹⁶⁹, M. Raymond ³⁶, A. L. Read ¹²⁵, N. P. Readioff ¹³⁹, D. M. Rebutzi ^{73a,73b}, G. Redlinger ²⁹

K. Reeves ,²⁶ J. A. Reidelsturz ,¹⁷¹ D. Reikher ,¹⁵¹ A. Rej ,¹⁴¹ C. Rembser ,³⁶ A. Renardi ,⁴⁸ M. Renda ,^{27b} M. B. Rendel ,¹¹⁰ F. Renner ,⁴⁸ A. G. Rennie ,⁵⁹ S. Resconi ,^{71a} M. Ressegotti ,^{57b,57a} E. D. Resseguie ,^{17a} S. Rettie ,³⁶ J. G. Reyes Rivera ,¹⁰⁷ B. Reynolds ,¹¹⁹ E. Reynolds ,^{17a} M. Rezaei Estabragh ,¹⁷¹ O. L. Rezanova ,³⁷ P. Reznicek ,¹³³ N. Ribaric ,⁹¹ E. Ricci ,^{78a,78b} R. Richter ,¹¹⁰ S. Richter ,^{47a,47b} E. Richter-Was ,^{85b} M. Ridel ,¹²⁷ S. Ridouani ,^{35d} P. Rieck ,¹¹⁷ P. Riedler ,³⁶ M. Rijssenbeek ,¹⁴⁵ A. Rimoldi ,^{73a,73b} M. Rimoldi ,⁴⁸ L. Rinaldi ,^{23b,23a} T. T. Rinn ,²⁹ M. P. Rinnagel ,¹⁰⁹ G. Ripellino ,¹⁶¹ I. Riu ,¹³ P. Rivadeneira ,⁴⁸ J. C. Rivera Vergara ,¹⁶⁵ F. Rizatdinova ,¹²¹ E. Rizvi ,⁹⁴ C. Rizzi ,⁵⁶ B. A. Roberts ,¹⁶⁷ B. R. Roberts ,^{17a} S. H. Robertson ,^{104,p} M. Robin ,⁴⁸ D. Robinson ,³² C. M. Robles Gajardo ,^{137f} M. Robles Manzano ,¹⁰⁰ A. Robson ,⁵⁹ A. Rocchi ,^{76a,76b} C. Roda ,^{74a,74b} S. Rodriguez Bosca ,^{63a} Y. Rodriguez Garcia ,^{22a} A. Rodriguez Rodriguez ,⁵⁴ A. M. Rodríguez Vera ,^{156b} S. Roe ,³⁶ J. T. Roemer ,¹⁶⁰ A. R. Roepe-Gier ,¹³⁶ J. Roggel ,¹⁷¹ O. Røhne ,¹²⁵ R. A. Rojas ,¹⁰³ C. P. A. Roland ,⁶⁸ J. Roloff ,²⁹ A. Romaniouk ,³⁷ E. Romano ,^{73a,73b} M. Romano ,^{23b} A. C. Romero Hernandez ,¹⁶² N. Rompotis ,⁹² L. Roos ,¹²⁷ S. Rosati ,^{75a} B. J. Rosser ,³⁹ E. Rossi ,¹²⁶ E. Rossi ,^{72a,72b} L. P. Rossi ,^{57b} L. Rossini ,⁴⁸ R. Rosten ,¹¹⁹ M. Rotaru ,^{27b} B. Rottler ,⁵⁴ C. Rougier ,^{102,af} D. Rousseau ,⁶⁶ D. Rouso ,³² A. Roy ,¹⁶² S. Roy-Garand ,¹⁵⁵ A. Rozanov ,¹⁰² Y. Rozen ,¹⁵⁰ X. Ruan ,^{33g} A. Rubio Jimenez ,¹⁶³ A. J. Ruby ,⁹² V. H. Ruelas Rivera ,¹⁸ T. A. Ruggeri ,¹ A. Ruggiero ,¹²⁶ A. Ruiz-Martinez ,¹⁶³ A. Rummler ,³⁶ Z. Rurikova ,⁵⁴ N. A. Rusakovich ,³⁸ H. L. Russell ,¹⁶⁵ J. P. Rutherford ,⁷ K. Rybacki ,⁹¹ M. Rybar ,¹³³ E. B. Rye ,¹²⁵ A. Ryzhov ,³⁷ J. A. Sabater Iglesias ,⁵⁶ P. Sabatini ,¹⁶³ L. Sabetta ,^{75a,75b} H.F.-W. Sadrozinski ,¹³⁶ F. Safai Tehrani ,^{75a} B. Safarzadeh Samani ,¹⁴⁶ M. Safdari ,¹⁴³ S. Saha ,¹⁰⁴ M. Sahinsoy ,¹¹⁰ M. Saimpert ,¹³⁵ M. Saito ,¹⁵³ T. Saito ,¹⁵³ D. Salamani ,³⁶ A. Salnikov ,¹⁴³ J. Salt ,¹⁶³ A. Salvador Salas ,¹³ D. Salvatore ,^{43b,43a} F. Salvatore ,¹⁴⁶ A. Salzburger ,³⁶ D. Sammel ,⁵⁴ D. Sampsonidis ,^{152,ac} D. Sampsonidou ,^{123,62c} J. Sánchez ,¹⁶³ A. Sanchez Pineda ,⁴ V. Sanchez Sebastian ,¹⁶³ H. Sandaker ,¹²⁵ C. O. Sander ,⁴⁸ J. A. Sandesara ,¹⁰³ M. Sandhoff ,¹⁷¹ C. Sandoval ,^{22b} D. P. C. Sankey ,¹³⁴ T. Sano ,⁸⁷ A. Sansoni ,⁵³ L. Santi ,^{75a,75b} C. Santoni ,⁴⁰ H. Santos ,^{130a,130b} S. N. Santpur ,^{17a} A. Santra ,¹⁶⁹ K. A. Saoucha ,¹³⁹ J. G. Saraiva ,^{130a,130d} J. Sardain ,⁷ O. Sasaki ,⁸³ K. Sato ,¹⁵⁷ C. Sauer ,^{63b} F. Sauerburger ,⁵⁴ E. Sauvan ,⁴ P. Savard ,^{155,d} R. Sawada ,¹⁵³ C. Sawyer ,¹³⁴ L. Sawyer ,⁹⁷ I. Sayago Galvan ,¹⁶³ C. Sbarra ,^{23b} A. Sbrizzi ,^{23b,23a} T. Scanlon ,⁹⁶ J. Schaarschmidt ,¹³⁸ P. Schacht ,¹¹⁰ D. Schaefer ,³⁹ U. Schäfer ,¹⁰⁰ A. C. Schaffer ,^{66,44} D. Schaile ,¹⁰⁹ R. D. Schamberger ,¹⁴⁵ E. Schanet ,¹⁰⁹ C. Scharf ,¹⁸ M. M. Schefer ,¹⁹ V. A. Schegelsky ,³⁷ D. Scheirich ,¹³³ F. Schenck ,¹⁸ M. Schernau ,¹⁶⁰ C. Scheulen ,⁵⁵ C. Schiavi ,^{57b,57a} E. J. Schioppa ,^{70a,70b} M. Schioppa ,^{43b,43a} B. Schlag ,^{143,u} K. E. Schleicher ,⁵⁴ S. Schlenker ,³⁶ J. Schmeing ,¹⁷¹ M. A. Schmidt ,¹⁷¹ K. Schmieden ,¹⁰⁰ C. Schmitt ,¹⁰⁰ S. Schmitt ,⁴⁸ L. Schoeffel ,¹³⁵ A. Schoening ,^{63b} P. G. Scholer ,⁵⁴ E. Schopf ,¹²⁶ M. Schott ,¹⁰⁰ J. Schovancova ,³⁶ S. Schramm ,⁵⁶ F. Schroeder ,¹⁷¹ H.-C. Schultz-Coulon ,^{63a} M. Schumacher ,⁵⁴ B. A. Schumm ,¹³⁶ Ph. Schune ,¹³⁵ A. J. Schuy ,¹³⁸ H. R. Schwartz ,¹³⁶ A. Schwartzman ,¹⁴³ T. A. Schwarz ,¹⁰⁶ Ph. Schwemling ,¹³⁵ R. Schwienhorst ,¹⁰⁷ A. Sciandra ,¹³⁶ G. Sciolla ,²⁶ F. Scuri ,^{74a} F. Scutti ,¹⁰⁵ C. D. Sebastiani ,⁹² K. Sedlaczek ,¹¹⁵ P. Seema ,¹⁸ S. C. Seidel ,¹¹² A. Seiden ,¹³⁶ B. D. Seidlitz ,⁴¹ C. Seitz ,⁴⁸ J. M. Seixas ,^{82b} G. Sekhniaidze ,^{72a} S. J. Sekula ,⁴⁴ L. Selem ,⁴ N. Semprini-Cesari ,^{23b,23a} S. Sen ,⁵¹ D. Sengupta ,⁵⁶ V. Senthilkumar ,¹⁶³ L. Serin ,⁶⁶ L. Serkin ,^{69a,69b} M. Sessa ,^{77a,77b} H. Severini ,¹²⁰ F. Sforza ,^{57b,57a} A. Sfyrila ,⁵⁶ E. Shabalina ,⁵⁵ R. Shaheen ,¹⁴⁴ J. D. Shahinian ,¹²⁸ D. Shaked Renous ,¹⁶⁹ L. Y. Shan ,^{14a} M. Shapiro ,^{17a} A. Sharma ,³⁶ A. S. Sharma ,¹⁶⁴ P. Sharma ,⁸⁰ S. Sharma ,⁴⁸ P. B. Shatalov ,³⁷ K. Shaw ,¹⁴⁶ S. M. Shaw ,¹⁰¹ Q. Shen ,^{62c,5} P. Sherwood ,⁹⁶ L. Shi ,⁹⁶ X. Shi ,^{14a} C. O. Shimmin ,¹⁷² Y. Shimogama ,¹⁶⁸ J. D. Shinner ,⁹⁵ I. P. J. Shipsey ,¹²⁶ S. Shirabe ,⁶⁰ M. Shiyakova ,^{38,ai} J. Shlomi ,¹⁶⁹ M. J. Shochet ,³⁹ J. Shojaii ,¹⁰⁵ D. R. Shope ,¹²⁵ S. Shrestha ,^{119,aj} E. M. Shrif ,^{33g} M. J. Shroff ,¹⁶⁵ P. Sicho ,¹³¹ A. M. Sickles ,¹⁶² E. Sideras Haddad ,^{33g} A. Sidoti ,^{23b} F. Siegert ,⁵⁰ Dj. Sijacki ,¹⁵ R. Sikora ,^{85a} F. Sili ,⁹⁰ J. M. Silva ,²⁰ M. V. Silva Oliveira ,³⁶ S. B. Silverstein ,^{47a} S. Simion ,⁶⁶ R. Simoniello ,³⁶ E. L. Simpson ,⁵⁹ H. Simpson ,¹⁴⁶ L. R. Simpson ,¹⁰⁶ N. D. Simpson ,⁹⁸ S. Simsek ,^{21d} S. Sindhu ,⁵⁵ P. Sinervo ,¹⁵⁵ S. Singh ,¹⁴² S. Singh

- A. Strubig^{47a,47b} S. A. Stucci²⁹ B. Stugu¹⁶ J. Stupak¹²⁰ N. A. Styles⁴⁸ D. Su¹⁴³ S. Su^{62a} W. Su^{62d,138,62c}
 X. Su^{62a,66} K. Sugizaki¹⁵³ V. V. Sulin³⁷ M. J. Sullivan⁹² D. M. S. Sultan^{78a,78b} L. Sultanaliyeva³⁷
 S. Sultansoy^{3b} T. Sumida⁸⁷ S. Sun¹⁰⁶ S. Sun¹⁷⁰ O. Sunneborn Gudnadottir¹⁶¹ M. R. Sutton¹⁴⁶ M. Svatos¹³¹
 M. Swiatlowski^{156a} T. Swirski¹⁶⁶ I. Sykora^{28a} M. Sykora¹³³ T. Sykora¹³³ D. Ta¹⁰⁰ K. Tackmann^{48,ak}
 A. Taffard¹⁶⁰ R. Tafirout^{156a} J. S. Tafoya Vargas⁶⁶ R. H. M. Taibah¹²⁷ R. Takashima⁸⁸ E. P. Takeva⁵²
 Y. Takubo⁸³ M. Talby¹⁰² A. A. Talyshv³⁷ K. C. Tam^{64b} N. M. Tamir¹⁵¹ A. Tanaka¹⁵³ J. Tanaka¹⁵³
 R. Tanaka⁶⁶ M. Tanasini^{57b,57a} Z. Tao¹⁶⁴ S. Tapia Araya^{137f} S. Tapprogge¹⁰⁰ A. Tarek Abouelfadl Mohamed¹⁰⁷
 S. Tarem¹⁵⁰ K. Tariq^{62b} G. Tarna^{102,27b} G. F. Tartarelli^{71a} P. Tas¹³³ M. Tasevsky¹³¹ E. Tassi^{43b,43a}
 A. C. Tate¹⁶² G. Tateno¹⁵³ Y. Tayalati^{35e,al} G. N. Taylor¹⁰⁵ W. Taylor^{156b} H. Teagle⁹² A. S. Tee¹⁷⁰
 R. Teixeira De Lima¹⁴³ P. Teixeira-Dias⁹⁵ J. J. Teoh¹⁵⁵ K. Terashi¹⁵³ J. Terron⁹⁹ S. Terzo¹³ M. Testa⁵³
 R. J. Teuscher^{155,p} A. Thaler⁷⁹ O. Theiner⁵⁶ N. Themistokleous⁵² T. Theveneaux-Pelzer¹⁰² O. Thielmann¹⁷¹
 D. W. Thomas⁹⁵ J. P. Thomas²⁰ E. A. Thompson^{17a} P. D. Thompson²⁰ E. Thomson¹²⁸ Y. Tian⁵⁵
 V. Tikhomirov^{37,1} Yu. A. Tikhonov³⁷ S. Timoshenko³⁷ E. X. L. Ting¹ P. Tipton¹⁷² S. H. Tlou^{33g} A. Tnourji⁴⁰
 K. Todome^{23b,23a} S. Todorova-Nova¹³³ S. Todt⁵⁰ M. Togawa⁸³ J. Tojo⁸⁹ S. Tokár^{28a} K. Tokushuku⁸³
 O. Toldaiev⁶⁸ R. Tombs³² M. Tomoto^{83,111} L. Tompkins^{143,u} K. W. Topolnicki^{85b} E. Torrence¹²³
 H. Torres^{102,af} E. Torró Pastor¹⁶³ M. Toscani³⁰ C. Tosciri³⁹ M. Tost¹¹ D. R. Tovey¹³⁹ A. Traet¹⁶
 I. S. Trandafir^{27b} T. Trefzger¹⁶⁶ A. Tricoli²⁹ I. M. Trigger^{156a} S. Trincaz-Duvoid¹²⁷ D. A. Trischuk²⁶
 B. Trocmé⁶⁰ C. Troncon^{71a} L. Truong^{33c} M. Trzebinski⁸⁶ A. Trzupke⁸⁶ F. Tsai¹⁴⁵ M. Tsai¹⁰⁶
 A. Tsiamis^{152,ac} P. V. Tsireshka³⁷ S. Tsigaridas^{156a} A. Tsirigotis^{152,ad} V. Tsiskaridze¹⁴⁵ E. G. Tskhadadze^{149a}
 M. Tsooulou^{152,ac} Y. Tsujikawa⁸⁷ I. I. Tsukerman³⁷ V. Tsulaia^{17a} S. Tsuno⁸³ O. Tsur¹⁵⁰ K. Tsurii¹¹⁸
 D. Tsybychev¹⁴⁵ Y. Tu^{64b} A. Tudorache^{27b} V. Tudorache^{27b} A. N. Tuna³⁶ S. Turchikhin³⁸ I. Turk Cakir^{3a}
 R. Turra^{71a} T. Turtuvshin^{38,am} P. M. Tuts⁴¹ S. Tzamarias^{152,ac} P. Tzani¹⁰ E. Tzovara¹⁰⁰ K. Uchida¹⁵³
 F. Ukegawa¹⁵⁷ P. A. Ulloa Poblete^{137c} E. N. Umaka²⁹ G. Unal³⁶ M. Unal¹¹ A. Undrus²⁹ G. Unel¹⁶⁰
 J. Urban^{28b} P. Urquijo¹⁰⁵ G. Usai⁸ R. Ushioda¹⁵⁴ M. Usman¹⁰⁸ Z. Uysal^{21b} L. Vacavant¹⁰² V. Vacek¹³²
 B. Vachon¹⁰⁴ K. O. H. Vadla¹²⁵ T. Vafeiadis³⁶ A. Vaitkus⁹⁶ C. Valderanis¹⁰⁹ E. Valdes Santurio^{47a,47b}
 M. Valente^{156a} S. Valentineti^{23b,23a} A. Valero¹⁶³ E. Valiente Moreno¹⁶³ A. Vallier^{102,af} J. A. Valls Ferrer¹⁶³
 D. R. Van Arneeman¹¹⁴ T. R. Van Daalen¹³⁸ P. Van Gemmeren⁶ M. Van Rijnbach^{125,36} S. Van Stroud⁹⁶
 I. Van Vulpen¹¹⁴ M. Vanadia^{76a,76b} W. Vandelli³⁶ M. Vandenbroucke¹³⁵ E. R. Vandewall¹²¹ D. Vannicola¹⁵¹
 L. Vannoli^{57b,57a} R. Vari^{75a} E. W. Varnes⁷ C. Varni^{17a} T. Varol¹⁴⁸ D. Varouchas⁶⁶ L. Varriale¹⁶³
 K. E. Varvell¹⁴⁷ M. E. Vasile^{27b} L. Vaslin⁴⁰ G. A. Vasquez¹⁶⁵ F. Vazeille⁴⁰ T. Vazquez Schroeder³⁶ J. Veatch³¹
 V. Vecchio¹⁰¹ M. J. Veen¹⁰³ I. Veliscek¹²⁶ L. M. Veloce¹⁵⁵ F. Veloso^{130a,130c} S. Veneziano^{75a} A. Ventura^{70a,70b}
 A. Verbytskyi¹¹⁰ M. Verducci^{74a,74b} C. Vergis²⁴ M. Verissimo De Araujo^{82b} W. Verkerke¹¹⁴ J. C. Vermeulen¹¹⁴
 C. Vernieri¹⁴³ P. J. Verschuuren⁹⁵ M. Vessella¹⁰³ M. C. Vetterli^{142,d} A. Vgenopoulos^{152,ac} N. Viaux Maira^{137f}
 T. Vickey¹³⁹ O. E. Vickey Boeriu¹³⁹ G. H. A. Viehhauser¹²⁶ L. Vigani^{63b} M. Villa^{23b,23a} M. Villaplana Perez¹⁶³
 E. M. Villhauer⁵² E. Vilucchi⁵³ M. G. Vincker³⁴ G. S. Virdee²⁰ A. Vishwakarma⁵² C. Vittori³⁶ I. Vivarelli¹⁴⁶
 V. Vladimirov¹⁶⁷ E. Voevodina¹¹⁰ F. Vogel¹⁰⁹ P. Vokac¹³² J. Von Ahnen⁴⁸ E. Von Toerne²⁴ B. Vormwald³⁶
 V. Vorobel¹³³ K. Vorobev³⁷ M. Vos¹⁶³ K. Voss¹⁴¹ J. H. Vosseveld⁹² M. Vozak¹¹⁴ L. Vozdecky⁹⁴
 N. Vranjes¹⁵ M. Vranjes Milosavljevic¹⁵ M. Vreeswijk¹¹⁴ R. Vuillermet³⁶ O. Vujanovic¹⁰⁰ I. Vukotic³⁹
 S. Wada¹⁵⁷ C. Wagner¹⁰³ J. M. Wagner^{17a} W. Wagner¹⁷¹ S. Wahdan¹⁷¹ H. Wahlberg⁹⁰ R. Wakasa¹⁵⁷
 M. Wakida¹¹¹ J. Walder¹³⁴ R. Walker¹⁰⁹ W. Walkowiak¹⁴¹ A. Wall¹²⁸ A. Z. Wang¹⁷⁰ C. Wang¹⁰⁰
 C. Wang^{62c} H. Wang^{17a} J. Wang^{64a} R.-J. Wang¹⁰⁰ R. Wang⁶¹ R. Wang⁶ S. M. Wang¹⁴⁸ S. Wang^{62b}
 T. Wang^{62a} W. T. Wang⁸⁰ X. Wang^{14c} X. Wang¹⁶² X. Wang^{62c} Y. Wang^{62d} Y. Wang^{14c} Z. Wang¹⁰⁶
 Z. Wang^{62d,51,62c} Z. Wang¹⁰⁶ A. Warburton¹⁰⁴ R. J. Ward²⁰ N. Warrack⁵⁹ A. T. Watson²⁰ H. Watson⁵⁹
 M. F. Watson²⁰ G. Watts¹³⁸ B. M. Waugh⁹⁶ C. Weber²⁹ H. A. Weber¹⁸ M. S. Weber¹⁹ S. M. Weber^{63a}
 C. Wei^{62a} Y. Wei¹²⁶ A. R. Weidberg¹²⁶ E. J. Weik¹¹⁷ J. Weingarten⁴⁹ M. Weirich¹⁰⁰ C. Weiser⁵⁴
 C. J. Wells⁴⁸ T. Wenaus²⁹ B. Wendland⁴⁹ T. Wengler³⁶ N. S. Wenke¹¹⁰ N. Wermes²⁴ M. Wessels^{63a}
 K. Whalen¹²³ A. M. Wharton⁹¹ A. S. White⁶¹ A. White⁸ M. J. White¹ D. Whiteson¹⁶⁰ L. Wickremasinghe¹²⁴
 W. Wiedenmann¹⁷⁰ C. M. Wiel⁵⁰ M. WIELERS¹³⁴ C. Wigglesworth⁴² L. A. M. Wiik-Fuchs⁵⁴ D. J. Wilbern¹²⁰
 H. G. Wilkens³⁶ D. M. Williams⁴¹ H. H. Williams¹²⁸ S. Williams³² S. Willocq¹⁰³ B. J. Wilson¹⁰¹
 P. J. Windischhofer³⁹ F. Winklmeier¹²³ B. T. Winter⁵⁴ J. K. Winter¹⁰¹ M. Wittgen¹⁴³ M. Wobisch⁹⁷
 R. Wölker¹²⁶ J. Wollrath¹⁶⁰ M. W. Wolter⁸⁶ H. Wolters^{130a,130c} V. W. S. Wong¹⁶⁴ A. F. Wongel⁴⁸ S. D. Worm⁴⁸
 B. K. Wosiek⁸⁶ K. W. Woźniak⁸⁶ K. Wraight⁵⁹ J. Wu^{14a,14e} M. Wu^{64a} M. Wu¹¹³ S. L. Wu¹⁷⁰ X. Wu⁵⁶
 Y. Wu^{62a} Z. Wu¹³⁵ J. Wuerzinger¹¹⁰ T. R. Wyatt¹⁰¹ B. M. Wynne⁵² S. Xella⁴² L. Xia^{14c} M. Xia^{14b}
 J. Xiang^{64c} X. Xiao¹⁰⁶ M. Xie^{62a} X. Xie^{62a} S. Xin^{14a,14e} J. Xiong^{17a} I. Xioutidis¹⁴⁶ D. Xu^{14a} H. Xu^{62a}
 H. Xu^{62a} L. Xu^{62a} R. Xu¹²⁸ T. Xu¹⁰⁶ Y. Xu^{14b} Z. Xu⁵² Z. Xu^{14a} B. Yabsley¹⁴⁷ S. Yacoob^{33a}
 N. Yamaguchi⁸⁹ Y. Yamaguchi¹⁵⁴ E. Yamashita¹⁵³ H. Yamauchi¹⁵⁷ T. Yamazaki^{17a} Y. Yamazaki⁸⁴ J. Yan^{62c}
 S. Yan¹²⁶ Z. Yan²⁵ H. J. Yang^{62c,62d} H. T. Yang^{62a} S. Yang^{62a} T. Yang^{64c} X. Yang^{62a} X. Yang^{14a}
 Y. Yang⁴⁴ Y. Yang^{62a} Z. Yang^{62a,106} W.-M. Yao^{17a} Y. C. Yap⁴⁸ H. Ye^{14c} H. Ye⁵⁵ J. Ye⁴⁴ S. Ye²⁹ X. Ye^{62a}

Y. Yeh⁹⁶, I. Yeletsikh³⁸, B. K. Yeo^{17a}, M. R. Yexley⁹¹, P. Yin⁴¹, K. Yorita¹⁶⁸, S. Younas^{27b}, C. J. S. Young⁵⁴,
 C. Young¹⁴³, Y. Yu^{62a}, M. Yuan¹⁰⁶, R. Yuan^{62b,an}, L. Yue⁹⁶, M. Zaazoua^{35e}, B. Zabinski⁸⁶, E. Zaid⁵²,
 T. Zakareishvili^{149b}, N. Zakharchuk³⁴, S. Zambito⁵⁶, J. A. Zamora Saa^{137d,137b}, J. Zang¹⁵³, D. Zanzi⁵⁴,
 O. Zaplatilek¹³², C. Zeitnitz¹⁷¹, H. Zeng^{14a}, J. C. Zeng¹⁶², D. T. Zenger, Jr.²⁶, O. Zenin³⁷, T. Ženiš^{28a}, S. Zenz⁹⁴,
 S. Zerradi^{35a}, D. Zerwas⁶⁶, M. Zhai^{14a,14e}, B. Zhang^{14c}, D. F. Zhang¹³⁹, J. Zhang^{62b}, J. Zhang⁶, K. Zhang^{14a,14e},
 L. Zhang^{14c}, P. Zhang^{14a,14e}, R. Zhang¹⁷⁰, S. Zhang¹⁰⁶, T. Zhang¹⁵³, X. Zhang^{62c}, X. Zhang^{62b}, Y. Zhang^{62c,5},
 Y. Zhang⁹⁶, Z. Zhang^{17a}, Z. Zhang⁶⁶, H. Zhao¹³⁸, P. Zhao⁵¹, T. Zhao^{62b}, Y. Zhao¹³⁶, Z. Zhao^{62a},
 A. Zhemchugov³⁸, K. Zheng¹⁶², X. Zheng^{62a}, Z. Zheng¹⁴³, D. Zhong¹⁶², B. Zhou¹⁰⁶, H. Zhou⁷, N. Zhou^{62c},
 Y. Zhou⁷, C. G. Zhu^{62b}, J. Zhu¹⁰⁶, Y. Zhu^{62c}, Y. Zhu^{62a}, X. Zhuang^{14a}, K. Zhukov³⁷, V. Zhulanov³⁷,
 N. I. Zimine³⁸, J. Zinsser^{63b}, M. Ziolkowski¹⁴¹, L. Živković¹⁵, A. Zoccoli^{23b,23a}, K. Zoch⁵⁶, T. G. Zorbas¹³⁹,
 O. Zormpa⁴⁶, W. Zou⁴¹ and L. Zwalinski³⁶

(ATLAS Collaboration)

¹*Department of Physics, University of Adelaide, Adelaide, Australia*

²*Department of Physics, University of Alberta, Edmonton, Alberta, Canada*

^{3a}*Department of Physics, Ankara University, Ankara, Türkiye*

^{3b}*Division of Physics, TOBB University of Economics and Technology, Ankara, Türkiye*

⁴*LAPP, Université Savoie Mont Blanc, CNRS/IN2P3, Annecy, France*

⁵*APC, Université Paris Cité, CNRS/IN2P3, Paris, France*

⁶*High Energy Physics Division, Argonne National Laboratory, Argonne, Illinois, USA*

⁷*Department of Physics, University of Arizona, Tucson, Arizona, USA*

⁸*Department of Physics, University of Texas at Arlington, Arlington, Texas, USA*

⁹*Physics Department, National and Kapodistrian University of Athens, Athens, Greece*

¹⁰*Physics Department, National Technical University of Athens, Zografou, Greece*

¹¹*Department of Physics, University of Texas at Austin, Austin, Texas, USA*

¹²*Institute of Physics, Azerbaijan Academy of Sciences, Baku, Azerbaijan*

¹³*Institut de Física d'Altes Energies (IFAE), Barcelona Institute of Science and Technology, Barcelona, Spain*

^{14a}*Institute of High Energy Physics, Chinese Academy of Sciences, Beijing, China*

^{14b}*Physics Department, Tsinghua University, Beijing, China*

^{14c}*Department of Physics, Nanjing University, Nanjing, China*

^{14d}*School of Science, Shenzhen Campus of Sun Yat-sen University, China*

^{14e}*University of Chinese Academy of Science (UCAS), Beijing, China*

¹⁵*Institute of Physics, University of Belgrade, Belgrade, Serbia*

¹⁶*Department for Physics and Technology, University of Bergen, Bergen, Norway*

^{17a}*Physics Division, Lawrence Berkeley National Laboratory, Berkeley, California, USA*

^{17b}*University of California, Berkeley, California, USA*

¹⁸*Institut für Physik, Humboldt Universität zu Berlin, Berlin, Germany*

¹⁹*Albert Einstein Center for Fundamental Physics and Laboratory for High Energy Physics, University of Bern, Bern, Switzerland*

²⁰*School of Physics and Astronomy, University of Birmingham, Birmingham, United Kingdom*

^{21a}*Department of Physics, Bogazici University, Istanbul, Türkiye*

^{21b}*Department of Physics Engineering, Gaziantep University, Gaziantep, Türkiye*

^{21c}*Department of Physics, Istanbul University, Istanbul, Türkiye*

^{21d}*Istinye University, Sariyer, Istanbul, Türkiye*

^{22a}*Facultad de Ciencias y Centro de Investigaciones, Universidad Antonio Nariño, Bogotá, Colombia*

^{22b}*Departamento de Física, Universidad Nacional de Colombia, Bogotá, Colombia*

^{23a}*Dipartimento di Fisica e Astronomia A. Righi, Università di Bologna, Bologna, Italy*

^{23b}*INFN Sezione di Bologna, Bologna, Italy*

²⁴*Physikalisches Institut, Universität Bonn, Bonn, Germany*

²⁵*Department of Physics, Boston University, Boston, Massachusetts, USA*

²⁶*Department of Physics, Brandeis University, Waltham, Massachusetts, USA*

^{27a}*Transilvania University of Brasov, Brasov, Romania*

^{27b}*Horia Hulubei National Institute of Physics and Nuclear Engineering, Bucharest, Romania*

^{27c}*Department of Physics, Alexandru Ioan Cuza University of Iasi, Iasi, Romania*

^{27d}*National Institute for Research and Development of Isotopic and Molecular Technologies, Physics Department, Cluj-Napoca, Romania*

^{27e}*University Politehnica Bucharest, Bucharest, Romania*

^{27f}*West University in Timisoara, Timisoara, Romania*

^{27g}*Faculty of Physics, University of Bucharest, Bucharest, Romania*

- ^{28a}*Faculty of Mathematics, Physics and Informatics, Comenius University, Bratislava, Slovak Republic*
- ^{28b}*Department of Subnuclear Physics, Institute of Experimental Physics of the Slovak Academy of Sciences, Kosice, Slovak Republic*
- ²⁹*Physics Department, Brookhaven National Laboratory, Upton, New York, USA*
- ³⁰*Universidad de Buenos Aires, Facultad de Ciencias Exactas y Naturales, Departamento de Física, y CONICET, Instituto de Física de Buenos Aires (IFIBA), Buenos Aires, Argentina*
- ³¹*California State University, California, USA*
- ³²*Cavendish Laboratory, University of Cambridge, Cambridge, United Kingdom*
- ^{33a}*Department of Physics, University of Cape Town, Cape Town, South Africa*
- ^{33b}*Themba Labs, Western Cape, South Africa*
- ^{33c}*Department of Mechanical Engineering Science, University of Johannesburg, Johannesburg, South Africa*
- ^{33d}*National Institute of Physics, University of the Philippines Diliman (Philippines), South Africa*
- ^{33e}*University of South Africa, Department of Physics, Pretoria, South Africa*
- ^{33f}*University of Zululand, KwaDlangezwa, South Africa*
- ^{33g}*School of Physics, University of the Witwatersrand, Johannesburg, South Africa*
- ³⁴*Department of Physics, Carleton University, Ottawa, Ontario, Canada*
- ^{35a}*Faculté des Sciences Ain Chock, Réseau Universitaire de Physique des Hautes Energies - Université Hassan II, Casablanca, Morocco*
- ^{35b}*Faculté des Sciences, Université Ibn-Tofail, Kénitra, Morocco*
- ^{35c}*Faculté des Sciences Semlalia, Université Cadi Ayyad, LPHEA-Marrakech, Morocco*
- ^{35d}*LPMR, Faculté des Sciences, Université Mohamed Premier, Oujda, Morocco*
- ^{35e}*Faculté des sciences, Université Mohammed V, Rabat, Morocco*
- ^{35f}*Institute of Applied Physics, Mohammed VI Polytechnic University, Ben Guerir, Morocco*
- ³⁶*CERN, Geneva, Switzerland*
- ³⁷*Affiliated with an institute covered by a cooperation agreement with CERN*
- ³⁸*Affiliated with an international laboratory covered by a cooperation agreement with CERN*
- ³⁹*Enrico Fermi Institute, University of Chicago, Chicago, Illinois, USA*
- ⁴⁰*LPC, Université Clermont Auvergne, CNRS/IN2P3, Clermont-Ferrand, France*
- ⁴¹*Nevis Laboratory, Columbia University, Irvington, New York, USA*
- ⁴²*Niels Bohr Institute, University of Copenhagen, Copenhagen, Denmark*
- ^{43a}*Dipartimento di Fisica, Università della Calabria, Rende, Italy*
- ^{43b}*INFN Gruppo Collegato di Cosenza, Laboratori Nazionali di Frascati, Italy*
- ⁴⁴*Physics Department, Southern Methodist University, Dallas, Texas, USA*
- ⁴⁵*Physics Department, University of Texas at Dallas, Richardson, Texas, USA*
- ⁴⁶*National Centre for Scientific Research “Demokritos”, Agia Paraskevi, Greece*
- ^{47a}*Department of Physics, Stockholm University, Sweden*
- ^{47b}*Oskar Klein Centre, Stockholm, Sweden*
- ⁴⁸*Deutsches Elektronen-Synchrotron DESY, Hamburg and Zeuthen, Germany*
- ⁴⁹*Fakultät Physik, Technische Universität Dortmund, Dortmund, Germany*
- ⁵⁰*Institut für Kern- und Teilchenphysik, Technische Universität Dresden, Dresden, Germany*
- ⁵¹*Department of Physics, Duke University, Durham, North Carolina, USA*
- ⁵²*SUPA - School of Physics and Astronomy, University of Edinburgh, Edinburgh, United Kingdom*
- ⁵³*INFN e Laboratori Nazionali di Frascati, Frascati, Italy*
- ⁵⁴*Physikalisches Institut, Albert-Ludwigs-Universität Freiburg, Freiburg, Germany*
- ⁵⁵*II. Physikalisches Institut, Georg-August-Universität Göttingen, Göttingen, Germany*
- ⁵⁶*Département de Physique Nucléaire et Corpusculaire, Université de Genève, Genève, Switzerland*
- ^{57a}*Dipartimento di Fisica, Università di Genova, Genova, Italy*
- ^{57b}*INFN Sezione di Genova, Genova, Italy*
- ⁵⁸*II. Physikalisches Institut, Justus-Liebig-Universität Giessen, Giessen, Germany*
- ⁵⁹*SUPA - School of Physics and Astronomy, University of Glasgow, Glasgow, United Kingdom*
- ⁶⁰*LPSC, Université Grenoble Alpes, CNRS/IN2P3, Grenoble INP, Grenoble, France*
- ⁶¹*Laboratory for Particle Physics and Cosmology, Harvard University, Cambridge, Massachusetts, USA*
- ^{62a}*Department of Modern Physics and State Key Laboratory of Particle Detection and Electronics, University of Science and Technology of China, Hefei, China*
- ^{62b}*Institute of Frontier and Interdisciplinary Science and Key Laboratory of Particle Physics and Particle Irradiation (MOE), Shandong University, Qingdao, China*
- ^{62c}*School of Physics and Astronomy, Shanghai Jiao Tong University, Key Laboratory for Particle Astrophysics and Cosmology (MOE), SKLPPC, Shanghai, China*
- ^{62d}*Tsung-Dao Lee Institute, Shanghai, China*
- ^{63a}*Kirchhoff-Institut für Physik, Ruprecht-Karls-Universität Heidelberg, Heidelberg, Germany*
- ^{63b}*Physikalisches Institut, Ruprecht-Karls-Universität Heidelberg, Heidelberg, Germany*

- ^{64a}*Department of Physics, Chinese University of Hong Kong, Shatin, N.T., Hong Kong, China*
- ^{64b}*Department of Physics, University of Hong Kong, Hong Kong, China*
- ^{64c}*Department of Physics and Institute for Advanced Study, Hong Kong University of Science and Technology, Clear Water Bay, Kowloon, Hong Kong, China*
- ⁶⁵*Department of Physics, National Tsing Hua University, Hsinchu, Taiwan*
- ⁶⁶*IJCLab, Université Paris-Saclay, CNRS/IN2P3, 91405 Orsay, France*
- ⁶⁷*Centro Nacional de Microelectrónica (IMB-CNM-CSIC), Barcelona, Spain*
- ⁶⁸*Department of Physics, Indiana University, Bloomington, Indiana, USA*
- ^{69a}*INFN Gruppo Collegato di Udine, Sezione di Trieste, Udine, Italy*
- ^{69b}*ICTP, Trieste, Italy*
- ^{69c}*Dipartimento Politecnico di Ingegneria e Architettura, Università di Udine, Udine, Italy*
- ^{70a}*INFN Sezione di Lecce, Italy*
- ^{70b}*Dipartimento di Matematica e Fisica, Università del Salento, Lecce, Italy*
- ^{71a}*INFN Sezione di Milano, Italy*
- ^{71b}*Dipartimento di Fisica, Università di Milano, Milano, Italy*
- ^{72a}*INFN Sezione di Napoli, Italy*
- ^{72b}*Dipartimento di Fisica, Università di Napoli, Napoli, Italy*
- ^{73a}*INFN Sezione di Pavia, Italy*
- ^{73b}*Dipartimento di Fisica, Università di Pavia, Pavia, Italy*
- ^{74a}*INFN Sezione di Pisa, Italy*
- ^{74b}*Dipartimento di Fisica E. Fermi, Università di Pisa, Pisa, Italy*
- ^{75a}*INFN Sezione di Roma, Italy*
- ^{75b}*Dipartimento di Fisica, Sapienza Università di Roma, Roma, Italy*
- ^{76a}*INFN Sezione di Roma Tor Vergata, Italy*
- ^{76b}*Dipartimento di Fisica, Università di Roma Tor Vergata, Roma, Italy*
- ^{77a}*INFN Sezione di Roma Tre, Italy*
- ^{77b}*Dipartimento di Matematica e Fisica, Università Roma Tre, Roma, Italy*
- ^{78a}*INFN-TIFPA, Italy*
- ^{78b}*Università degli Studi di Trento, Trento, Italy*
- ⁷⁹*Department of Astro and Particle Physics, Universität Innsbruck, Innsbruck, Austria*
- ⁸⁰*University of Iowa, Iowa City, Iowa, USA*
- ⁸¹*Department of Physics and Astronomy, Iowa State University, Ames, Iowa, USA*
- ^{82a}*Departamento de Engenharia Elétrica, Universidade Federal de Juiz de Fora (UFJF), Juiz de Fora, Brazil*
- ^{82b}*Universidade Federal do Rio De Janeiro COPPE/EE/IF, Rio de Janeiro, Brazil*
- ^{82c}*Instituto de Física, Universidade de São Paulo, São Paulo, Brazil*
- ^{82d}*Rio de Janeiro State University, Rio de Janeiro, Brazil*
- ⁸³*KEK, High Energy Accelerator Research Organization, Tsukuba, Japan*
- ⁸⁴*Graduate School of Science, Kobe University, Kobe, Japan*
- ^{85a}*AGH University of Science and Technology, Faculty of Physics and Applied Computer Science, Krakow, Poland*
- ^{85b}*Marian Smoluchowski Institute of Physics, Jagiellonian University, Krakow, Poland*
- ⁸⁶*Institute of Nuclear Physics Polish Academy of Sciences, Krakow, Poland*
- ⁸⁷*Faculty of Science, Kyoto University, Kyoto, Japan*
- ⁸⁸*Kyoto University of Education, Kyoto, Japan*
- ⁸⁹*Research Center for Advanced Particle Physics and Department of Physics, Kyushu University, Fukuoka, Japan*
- ⁹⁰*Instituto de Física La Plata, Universidad Nacional de La Plata and CONICET, La Plata, Argentina*
- ⁹¹*Physics Department, Lancaster University, Lancaster, United Kingdom*
- ⁹²*Oliver Lodge Laboratory, University of Liverpool, Liverpool, United Kingdom*
- ⁹³*Department of Experimental Particle Physics, Jožef Stefan Institute and Department of Physics, University of Ljubljana, Ljubljana, Slovenia*
- ⁹⁴*School of Physics and Astronomy, Queen Mary University of London, London, United Kingdom*
- ⁹⁵*Department of Physics, Royal Holloway University of London, Egham, United Kingdom*
- ⁹⁶*Department of Physics and Astronomy, University College London, London, United Kingdom*
- ⁹⁷*Louisiana Tech University, Ruston, Louisiana, USA*
- ⁹⁸*Fysiska institutionen, Lunds universitet, Lund, Sweden*
- ⁹⁹*Departamento de Física Teórica C-15 and CIAFF, Universidad Autónoma de Madrid, Madrid, Spain*
- ¹⁰⁰*Institut für Physik, Universität Mainz, Mainz, Germany*
- ¹⁰¹*School of Physics and Astronomy, University of Manchester, Manchester, United Kingdom*
- ¹⁰²*CPPM, Aix-Marseille Université, CNRS/IN2P3, Marseille, France*
- ¹⁰³*Department of Physics, University of Massachusetts, Amherst, Massachusetts, USA*
- ¹⁰⁴*Department of Physics, McGill University, Montreal, Quebec, Canada*

- ¹⁰⁵*School of Physics, University of Melbourne, Victoria, Australia*
- ¹⁰⁶*Department of Physics, University of Michigan, Ann Arbor, Michigan, USA*
- ¹⁰⁷*Department of Physics and Astronomy, Michigan State University, East Lansing, Michigan, USA*
- ¹⁰⁸*Group of Particle Physics, University of Montreal, Montreal, Quebec, Canada*
- ¹⁰⁹*Fakultät für Physik, Ludwig-Maximilians-Universität München, München, Germany*
- ¹¹⁰*Max-Planck-Institut für Physik (Werner-Heisenberg-Institut), München, Germany*
- ¹¹¹*Graduate School of Science and Kobayashi-Maskawa Institute, Nagoya University, Nagoya, Japan*
- ¹¹²*Department of Physics and Astronomy, University of New Mexico, Albuquerque, New Mexico, USA*
- ¹¹³*Institute for Mathematics, Astrophysics and Particle Physics, Radboud University/Nikhef, Nijmegen, Netherlands*
- ¹¹⁴*Nikhef National Institute for Subatomic Physics and University of Amsterdam, Amsterdam, Netherlands*
- ¹¹⁵*Department of Physics, Northern Illinois University, DeKalb, Illinois, USA*
- ^{116a}*New York University Abu Dhabi, Abu Dhabi*
- ^{116b}*University of Sharjah, Sharjah, United Arab Emirates*
- ¹¹⁷*Department of Physics, New York University, New York, New York, USA*
- ¹¹⁸*Ochanomizu University, Otsuka, Bunkyo-ku, Tokyo, Japan*
- ¹¹⁹*Ohio State University, Columbus, Ohio, USA*
- ¹²⁰*Homer L. Dodge Department of Physics and Astronomy, University of Oklahoma, Norman, Oklahoma, USA*
- ¹²¹*Department of Physics, Oklahoma State University, Stillwater, Oklahoma, USA*
- ¹²²*Palacký University, Joint Laboratory of Optics, Olomouc, Czech Republic*
- ¹²³*Institute for Fundamental Science, University of Oregon, Eugene, Oregon, USA*
- ¹²⁴*Graduate School of Science, Osaka University, Osaka, Japan*
- ¹²⁵*Department of Physics, University of Oslo, Oslo, Norway*
- ¹²⁶*Department of Physics, Oxford University, Oxford, United Kingdom*
- ¹²⁷*LPNHE, Sorbonne Université, Université Paris Cité, CNRS/IN2P3, Paris, France*
- ¹²⁸*Department of Physics, University of Pennsylvania, Philadelphia, Pennsylvania, USA*
- ¹²⁹*Department of Physics and Astronomy, University of Pittsburgh, Pittsburgh, Pennsylvania, USA*
- ^{130a}*Laboratório de Instrumentação e Física Experimental de Partículas - LIP, Lisboa, Portugal*
- ^{130b}*Departamento de Física, Faculdade de Ciências, Universidade de Lisboa, Lisboa, Portugal*
- ^{130c}*Departamento de Física, Universidade de Coimbra, Coimbra, Portugal*
- ^{130d}*Centro de Física Nuclear da Universidade de Lisboa, Lisboa, Portugal*
- ^{130e}*Departamento de Física, Universidade do Minho, Braga, Portugal*
- ^{130f}*Departamento de Física Teórica y del Cosmos, Universidad de Granada, Granada (Spain), Portugal*
- ^{130g}*Departamento de Física, Instituto Superior Técnico, Universidade de Lisboa, Lisboa, Portugal*
- ¹³¹*Institute of Physics of the Czech Academy of Sciences, Prague, Czech Republic*
- ¹³²*Czech Technical University in Prague, Prague, Czech Republic*
- ¹³³*Charles University, Faculty of Mathematics and Physics, Prague, Czech Republic*
- ¹³⁴*Particle Physics Department, Rutherford Appleton Laboratory, Didcot, United Kingdom*
- ¹³⁵*IRFU, CEA, Université Paris-Saclay, Gif-sur-Yvette, France*
- ¹³⁶*Santa Cruz Institute for Particle Physics, University of California Santa Cruz, Santa Cruz, California, USA*
- ^{137a}*Departamento de Física, Pontificia Universidad Católica de Chile, Santiago, Chile*
- ^{137b}*Millennium Institute for Subatomic physics at high energy frontier (SAPHIR), Santiago, Chile*
- ^{137c}*Instituto de Investigación Multidisciplinario en Ciencia y Tecnología, y Departamento de Física, Universidad de La Serena, Chile*
- ^{137d}*Universidad Andres Bello, Department of Physics, Santiago, Chile*
- ^{137e}*Instituto de Alta Investigación, Universidad de Tarapacá, Arica, Chile*
- ^{137f}*Departamento de Física, Universidad Técnica Federico Santa María, Valparaíso, Chile*
- ¹³⁸*Department of Physics, University of Washington, Seattle, Washington, USA*
- ¹³⁹*Department of Physics and Astronomy, University of Sheffield, Sheffield, United Kingdom*
- ¹⁴⁰*Department of Physics, Shinshu University, Nagano, Japan*
- ¹⁴¹*Department Physik, Universität Siegen, Siegen, Germany*
- ¹⁴²*Department of Physics, Simon Fraser University, Burnaby, British Columbia, Canada*
- ¹⁴³*SLAC National Accelerator Laboratory, Stanford, California, USA*
- ¹⁴⁴*Department of Physics, Royal Institute of Technology, Stockholm, Sweden*
- ¹⁴⁵*Departments of Physics and Astronomy, Stony Brook University, Stony Brook, New York, USA*
- ¹⁴⁶*Department of Physics and Astronomy, University of Sussex, Brighton, United Kingdom*
- ¹⁴⁷*School of Physics, University of Sydney, Sydney, Australia*
- ¹⁴⁸*Institute of Physics, Academia Sinica, Taipei, Taiwan*
- ^{149a}*E. Andronikashvili Institute of Physics, Iv. Javakhishvili Tbilisi State University, Tbilisi, Georgia*
- ^{149b}*High Energy Physics Institute, Tbilisi State University, Tbilisi, Georgia*
- ^{149c}*University of Georgia, Tbilisi, Georgia*

- ¹⁵⁰*Department of Physics, Technion, Israel Institute of Technology, Haifa, Israel*
- ¹⁵¹*Raymond and Beverly Sackler School of Physics and Astronomy, Tel Aviv University, Tel Aviv, Israel*
- ¹⁵²*Department of Physics, Aristotle University of Thessaloniki, Thessaloniki, Greece*
- ¹⁵³*International Center for Elementary Particle Physics and Department of Physics, University of Tokyo, Tokyo, Japan*
- ¹⁵⁴*Department of Physics, Tokyo Institute of Technology, Tokyo, Japan*
- ¹⁵⁵*Department of Physics, University of Toronto, Toronto, Ontario, Canada*
- ^{156a}*TRIUMF, Vancouver, British Columbia, Canada*
- ^{156b}*Department of Physics and Astronomy, York University, Toronto, Ontario, Canada*
- ¹⁵⁷*Division of Physics and Tomonaga Center for the History of the Universe, Faculty of Pure and Applied Sciences, University of Tsukuba, Tsukuba, Japan*
- ¹⁵⁸*Department of Physics and Astronomy, Tufts University, Medford, Massachusetts, USA*
- ¹⁵⁹*United Arab Emirates University, Al Ain, United Arab Emirates*
- ¹⁶⁰*Department of Physics and Astronomy, University of California Irvine, Irvine, California, USA*
- ¹⁶¹*Department of Physics and Astronomy, University of Uppsala, Uppsala, Sweden*
- ¹⁶²*Department of Physics, University of Illinois, Urbana, Illinois, USA*
- ¹⁶³*Instituto de Física Corpuscular (IFIC), Centro Mixto Universidad de Valencia - CSIC, Valencia, Spain*
- ¹⁶⁴*Department of Physics, University of British Columbia, Vancouver, British Columbia, Canada*
- ¹⁶⁵*Department of Physics and Astronomy, University of Victoria, Victoria, British Columbia, Canada*
- ¹⁶⁶*Fakultät für Physik und Astronomie, Julius-Maximilians-Universität Würzburg, Würzburg, Germany*
- ¹⁶⁷*Department of Physics, University of Warwick, Coventry, United Kingdom*
- ¹⁶⁸*Waseda University, Tokyo, Japan*
- ¹⁶⁹*Department of Particle Physics and Astrophysics, Weizmann Institute of Science, Rehovot, Israel*
- ¹⁷⁰*Department of Physics, University of Wisconsin, Madison, Wisconsin, USA*
- ¹⁷¹*Fakultät für Mathematik und Naturwissenschaften, Fachgruppe Physik, Bergische Universität Wuppertal, Wuppertal, Germany*
- ¹⁷²*Department of Physics, Yale University, New Haven, Connecticut, USA*

^aAlso at Department of Physics, King's College London, London, United Kingdom.

^bAlso at Institute of Physics, Azerbaijan Academy of Sciences, Baku, Azerbaijan.

^cAlso at Lawrence Livermore National Laboratory, Livermore, California, USA.

^dAlso at TRIUMF, Vancouver, British Columbia, Canada.

^eAlso at Department of Physics, University of Thessaly, Volos, Greece.

^fAlso at An-Najah National University, Nablus, Palestine.

^gAlso at Department of Physics, University of Fribourg, Fribourg, Switzerland.

^hAlso at Department of Physics, University of Colorado Boulder, Boulder, Colorado, USA.

ⁱDeceased.

^jAlso at Department of Physics, Westmont College, Santa Barbara, California, USA.

^kAlso at Departament de Física de la Universitat Autònoma de Barcelona, Barcelona, Spain.

^lAlso Affiliated with an institute covered by a cooperation agreement with CERN.

^mAlso at The Collaborative Innovation Center of Quantum Matter (CICQM), Beijing, China.

ⁿAlso at Department of Physics, Ben Gurion University of the Negev, Beer Sheva, Israel.

^oAlso at Università di Napoli Parthenope, Napoli, Italy.

^pAlso at Institute of Particle Physics (IPP), Victoria, British Columbia, Canada.

^qAlso at Bruno Kessler Foundation, Trento, Italy.

^rAlso at Borough of Manhattan Community College, City University of New York, New York, New York, USA.

^sAlso at National Institute of Physics, University of the Philippines Diliman (Philippines), Philippines.

^tAlso at Department of Financial and Management Engineering, University of the Aegean, Chios, Greece.

^uAlso at Department of Physics, Stanford University, Stanford, California, USA.

^vAlso at Centro Studi e Ricerche Enrico Fermi, Rome, Italy.

^wAlso at Department of Physics, California State University, East Bay, California, USA.

^xAlso at Institutio Catalana de Recerca i Estudis Avancats, ICREA, Barcelona, Spain.

^yAlso at Technical University of Munich, Munich, Germany.

^zAlso at Physics Department, Yeditepe University, Istanbul, Türkiye.

^{aa}Also at Institute of Theoretical Physics, Ilia State University, Tbilisi, Georgia.

^{ab}Also at CERN, Geneva, Switzerland.

^{ac}Also at Center for Interdisciplinary Research and Innovation (CIRI-AUTH), Thessaloniki, Greece.

^{ad}Also at Hellenic Open University, Patras, Greece.

^{ae}Also at Center for High Energy Physics, Peking University, China.

^{af}Also at L2IT, Université de Toulouse, CNRS/IN2P3, UPS, Toulouse, France.

^{ag}Also at Department of Physics, California State University, Sacramento, California, USA.

^{ah}Also at Département de Physique Nucléaire et Corpusculaire, Université de Genève, Genève, Switzerland.

^{ai}Also at Institute for Nuclear Research and Nuclear Energy (INRNE) of the Bulgarian Academy of Sciences, Sofia, Bulgaria.

^{aj}Also at Washington College, Chestertown, Maryland, USA.

^{ak}Also at Institut für Experimentalphysik, Universität Hamburg, Hamburg, Germany.

^{al}Also at Institute of Applied Physics, Mohammed VI Polytechnic University, Ben Guerir, Morocco.

^{am}Also at Institute of Physics and Technology, Ulaanbaatar, Mongolia.

^{an}Also at Department of Physics and Astronomy, Michigan State University, East Lansing, Michigan, USA.